1970

Authigenic analcite in the Golden Valley Formation southwestern North Dakota

Marvin J. Furman
University of North Dakota

Authentic Analcite in the Golden Valley Formation (?),

SouthWestern North Dakota

by

Marvin J. Furman

Bachelor of Science, St. Lawrence University 1965

A Thesis

Submitted to the Faculty

of the

University of North Dakota

in partial fulfillment of the requirements

for the degree of

Master of Science

Grand Forks, North Dakota

July
1970

This thesis submitted by Melvin J. Brekke in partial fulfillment of the requirements for the Degree of Master of Science from the University of North Dakota is hereby approved by the Faculty Advisory Committee under whom the work has been done.

_____
(Chairman)

_____

_____

_____
Dean of the Graduate School

Title: Authigenic Minerals in the Golden Valley Formation (?), South-
western North Dakota

Department: Geology

Degree: Master of Science

In presenting this thesis in partial fulfillment of the require-
ments for a graduate degree from the University of North Dakota, I a-
gree that the Library of this University shall make it freely available
for inspection. I further agree that permission for extensive copying
for scholarly purposes may be granted by the professor who supervised
my thesis work or, in his absence, by the Chairman of the Department
or the Dean of the Graduate School. It is understood that any copying
or publication or other use of this thesis or part thereof for financial
gain shall not be allowed without my written permission. It is also
understood that due recognition be given to me and to the University
of North Dakota in any scholarly use which may be made of any material
in my thesis.

Morris J. Furman

July 30, 1970

ACKNOWLEDGEMENTS

TABLE OF CONTENTS

LIST OF TABLES

LIST OF FIGURES

viii

Authigenic analcite constitutes up to about 60 percent of a massive, arkosic sandstone exposed on major buttes in the North Dakota Badlands. The analcite constitutes up to about 80 percent of a thin analcimolite bed at the top of the arkose unit. The analcite occurs as spherulites in the interstices of the arkose and as a cement in the analcimolite. Three types of spherulites are recognized: (1) spherulites with an internal radial structure; (2) spherulites with a massive center and a peripheral radial structure; and (3) spherulites lacking an internal radial structure or having a poorly-defined internal structure. The spherulites occur individually and as coalesced masses. Analcite in the arkose and analcimolite is silica-poor.

Detrital minerals associated with the analcite include quartz, plagioclase, K-feldspar, and illite. Sericite is associated with analcite in the arkose, and may also be authigenic. The analcite is least abundant at the base of the arkose unit and increases upward. The abundances of analcite and the detrital feldspars are inversely related.

Analcite composition, distribution with respect to the feldspars, presence of sericite, and the absence of a vitroclastic texture, suggests that analcite in the arkose was derived from post-depositional dissolution of the feldspars. It is proposed that analcite in the arkose and analcimolite were derived from different, but similar, parent materials.

MODES OF OCCURRENCE OF ANALCITE

Analcite is classified as a member of the zeolite group, although in structure, chemistry, and (igneous) paragenesis it has close affinities with the feldspathoids (Deer, et al., 1963). The composition of analcite is generally expressed as $NaAlSi_2O_6 \cdot nH_2O$. There are, however, variations in composition, in which potassium substitutes for sodium, and sodium and aluminum substitute for silicon (Wilkinson, 1968).

Analcite occurs in igneous and sedimentary rocks. It is a primary mineral of late formation in some intermediate and basic igneous rocks. It also forms in the late stages of crystallization of some hydrothermal solutions. In sedimentary rocks it occurs as icositetrahedral crystals, spherulites, and most frequently as replacements of volcanic glass shards.

Proposed origins for analcite in sedimentary rocks are by: (1) alteration of volcanic glass by hydrolysis (Bradley, 1929; Deffeyes, 1959); (2) direct precipitation from surface waters (Van Houten, 1962) (3) reaction and alteration of other alkali zeolites (Goodwin and Surdam, 1967); (4) reaction between saline waters and clay minerals (Keller, 1952); and (5) reaction and alteration of primary tectosilicate minerals (Hay, 1966).

Zeolites are among the most common authigenic silicate minerals in sedimentary rocks (Hay, 1966), usually forming in sediments as a product of diagenetic processes. Diagenesis, generally, is defined as the physical and chemical adjustment of the sediment after deposition, re-

sulting in changes in composition and texture. Diagenesis is restrict-
ed to lower temperatures and pressures to distinguish it from meta-
morphism. A number of mineralogical changes mark the transition from
diagenesis to low-grade metamorphism, among which is the replacement
of analcite by albite and quartz (Turner, 1958).

Pettijohn (1957) includes in diagenesis the processes of cementa-
tion, authigenesis, diagenetic differentiation, intrastratal solution,
and compaction. Cementation is the precipitation of mineral matter in
the voids of a clastic sediment, resulting in induration of the sedi-
ment to a rock. Authigenesis is the result of reaction among the con-
stituents of a sediment after deposition, with the formation of new
minerals or overgrowths on others already present. It is an attempt
to establish an equilibrium mineral assemblage. However, diagenetic
reactions, responsible for the elimination of unstable minerals, seldom
reach completion because of the low temperature conditions (Packham and
Crook, 1960). A typical diagenetic mineral assemblage, therefore, is
a disequilibrium assemblage, consisting of detrital "reactant" minerals
(or metastable authigenic minerals) and "product" authigenic minerals.
Diagenic differentiation is the redistribution of materials within a
sediment. Intrastratal solution is a chemical attrition by solutions
acting on the constituents of a rock after deposition. Compaction re-
duces or eliminates interstitial voids in a sediment, generally in-
creasing with greater depth of burial.

SCOPE AND PURPOSE OF STUDY

Zeolites are considered to be possible indicators of physical and

chemical conditions in diagenesis and low-grade metamorphism. Their importance has been evaluated by examining their natural occurrences, from which environmental parameters have been inferred. The inferred parameters have then been evaluated and more rigorously defined in experimental studies. Notable contributions to this approach have been made by Coombs (1954) and Coombs, et al. (1959).

Various aspects of the conditions under which zeolites crystallize have been recognized through extensive examinations of natural occurrences. This study is another contribution to the overall analysis. A major occurrence of analcite in a single rock unit was selected for study. Occurrences of analcite with respect to associated detrital and authigenic minerals, distribution in the rock unit, and composition have been investigated.

PREVIOUS INVESTIGATIONS

In North Dakota analcite was first reported in Tertiary rocks associated with uranium (Beroni and Bauer, 1952). Other occurrences in Tertiary rocks have been reported in South Dakota and Montana (Wanless, 1922; Rozendal, 1956; Denson, et al., 1959; Denson and Gill, 1965). These occurrences have been attributed to the alteration of associated tuffaceous materials.

DESCRIPTION OF STUDY AREA

The study area, in southwestern North Dakota, is situated between 102° to 104° W longitude and 46° to 48° N latitude. It includes isolated buttes in Golden Valley, Billings, Stark, Slope, and Dunn Coun-

ties (Fig. 1). The area covers approximately 150 square miles. Buttes, consisting of nearly horizontal beds of sand, silt, and clay, rise 400 to 600 feet above the plain. The topography of the area, to which the term "Badlands" is applied, is due mainly to stream and rain erosion. The area is drained by the Little Missouri River and its tributaries.

Figure 1.   Reference Map

SCALE

5   0   5   10 miles

N

○ ANALYZED SAMPLE LOCALITY (NUMBERED LOCALITIES REFER TO APPENDIX)

NORTH DAKOTA

Kildeer Mountains

DUNN COUNTY

GOLDEN VALLEY COUNTY

BILLINGS COUNTY

LITTLE MISSOURI RIVER

Flat Top Butte

Sentinel Butte

Bullion Butte

STARK COUNTY

SLOPE COUNTY

HT Butte

Chalky Buttes

Slide Butte
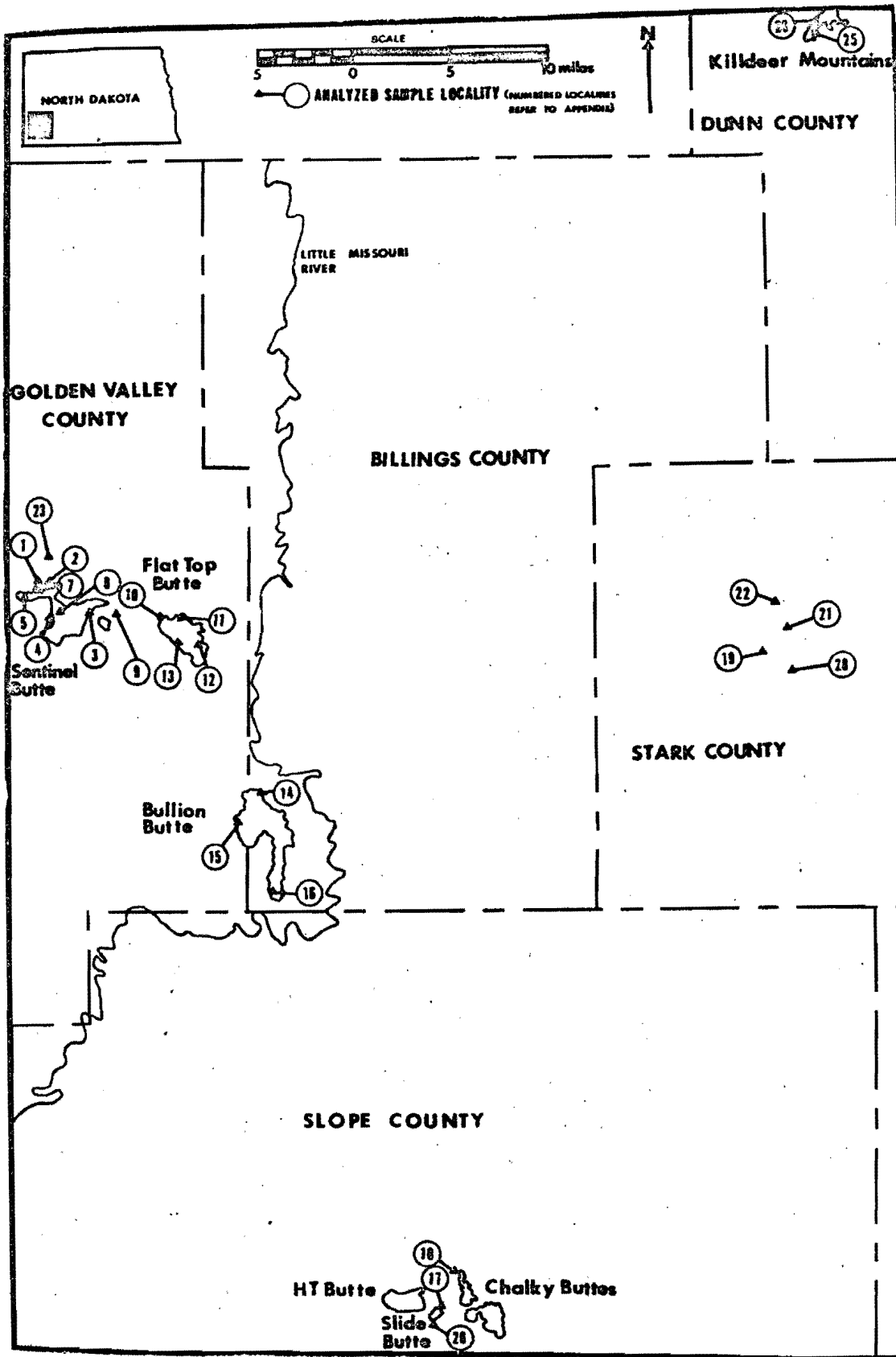
METHODS OF INVESTIGATION

SAMPLING

Tertiary rocks in southwestern North Dakota have been sampled to determine the occurrence of authigenic analcite. A total of 252 spot samples were taken. Analcite could not be distinguished in hand specimen and was identified by x-ray diffraction analysis. This required sampling to be carried out in two stages. First, reconnaissance sampling was undertaken to determine the distribution and major occurrences of analcite-bearing rocks. The analcite-bearing rocks were then sampled in detail. Factors influencing the choice of sample localities included the coourrence of complete sections, outcrops showing variations in lithology, and sedimentary structures. Sections more than ten feet thick were spot sampled at five-foot intervals from the top of the unit. Sections less than ten feet thick were sampled at the base, middle and top. Selected oriented samples were taken from sedimentary structures. Areal locations and stratigraphic positions of samples cited in this paper are given in the appendix and Figure 1.

ANALYTICAL PROCEDURES

General

The analcite-bearing rocks were examined in thin section to determine the characteristics, occurrence, and textural relationships of the detrital and authigenic minerals. X-ray diffraction methods were used for qualitative and semi-quantitative mineral analysis. Grain-

size distribution was determined by sieve and pipette analysis.

Petrographic Preparation

The majority of analcite-bearing rocks used for thin sectioning were friable and required special treatment. The samples were cut into slabs measuring approximately 1 X 3/4 X 1/8 inches and impregnated using a technique developed by Renton (1965).

Petrographic and Optical Measurements

Thirty-one thin sections were examined. An ocular micrometer was used for grain-size measurements. Grain shape was estimated by visual comparison with a roundness-sphericity chart (Krumbein and Sloss, 1963). Index of refraction was determined by the Becke line method. The composition of plagioclase in thin section was determined by Wahlstrom's procedure (1960). Extinction angles, measured with respect to appropriate cleavage planes, were plotted on a determinative curve from which the molecular percent of anorthite was read (Wahlstrom, 1960, pp. 120-125). Extinction angles were measured from the trace of {010} in fragments cut paralled to {001} , from the trace of {010} in sections cut normal to {001} and {010} and from the trace of the {010} plane in sections showing albite twinning or {010} cleavage.

X-Ray Diffraction Analysis

Procedures for X-ray Diffraction Analysis--194 samples were selected for routine qualitative and semi-quantitative x-ray diffraction analysis. A sample measuring approximately 6 X 4 X 4 inches was crushed and a 20 gram sub-sample was taken. The sub-sample was ground

in a 8000 Spex Mixer/Mill in Spex vial 8001 for seven minutes. A second sub-sample of 150 mg. was taken and ground in Spex vial 5004 for an additional seven minutes. One gram of the sample was then back-loaded in a cylindrical, rotating sample holder. The following machine conditions were used:

X-Ray Generator (Phillips Constant Potential 50 KV-50 ma).

X-Ray Tube (Machlett Cu Tube-Short Anode) 37 KV-18 ma.

Diffractometer (Phillips High Angle)

1 degree 2 Θ scan speed.

1 degree divergence and anti-scatter slit.

Ni filter.

Detector (Phillips Scintillation-Transistorized) 1.0 KV.

Circuit Panel (Phillips 12206/53), Bristol Recorder.

PHA, width 3.5V, level 6.0V.

Linear scale.

1 second time constant.

2×10^3 counts per second.

30 inches per hour chart speed.

Minerals were identified by peak position and relative intensity on the diffractogram. Diffractograms of reference minerals and the ASTM File were used for reference.

Modal compositions were semi-quantitatively determined by the method developed by Alexander and Klug (1948) and modified by Leroux, et al. (1953) and Karner (1968). The weight fraction of a given mineral component was calculated from the expression:

$$X_1 = \frac{I}{(I)} \cdot \frac{\mu_s^*}{\mu_1^*}$$

where,

X = weight fraction of component 1.

μ_1^* = mass absorption coefficient of component 1.

μ_s^* = mass absorption coefficient of bulk sample.

I = intensity diffracted at a definite Bragg angle 2θ by crystalline component 1 in the bulk sample.

(I) = intensity diffracted at a definite Bragg angle 2θ by pure crystalline component 1.

The equation expresses the weight fraction of a mineral component in the bulk sample as a ratio of the peak intensity of the mineral component to the peak intensity of a pure standard mineral, corrected for absorption. Leroux, et al. (1963) further established the following relationship to experimentally determine the absorption correction:

$$\frac{\mu_s^*}{\mu_1^*} = \frac{\rho_1 \log T_s/T_o}{\rho_s \log T_1/T_o}$$

where,

ρ_1 = apparent density of a pure sample of component 1.

ρ_s = apparent density of a sample containing weight fraction X of component 1.

T_o = intensity of incident x-ray beam.

T_s = intensity transmitted by sample containing weight fraction X of component 1.

T_1 = intensity transmitted by pure component 1.

Measurements were made of the peak intensity of a given component in the bulk sample and corresponding intensity of the pure com-

ponent. The peak intensity of the component in the bulk sample was determined by the difference between the peak height and background intensity. Values for the mass absorption coefficients of the minerals were taken from Tatlock (1966) or calculated from the data of Klug and Alexander (1954). The values used for the calculation of the weight fractions are given in Table 1. The results of these analyses are given in Tables 9, 10, 11, and 12, and Figures 9 and 14.

Precision and Accuracy of Semi-Quantitative X-Ray Diffraction
Mineral Analysis—Expressing the results of the analyses as semi-quantitative rather than quantitative implies a lesser degree of accuracy. Error has been introduced by using standards for measurement of 100 percent peak intensity that are not from the sample (standards

TABLE 1.   VALUES USED FOR THE CALCULATION OF MODAL COMPOSITIONS

UND Specimen	Mineral Standard	Peak Position 2θ	100 percent Intensity (counts per second)	Mass Absorption Coefficient
33	Quartz	20.9	1200	35
825	Potassium Feldspar	27.5	1640	49
4374	Sodium Plagioclase	28.0	2800	34
2506	Analcite	15.9	1604	34
2382	Muscovite	17.8	900	43
	*Total Clay	19.9	190	36
	Bulk Sample (μ_s^m)			40

* Clay fraction standard separated from samples

taken from U. N. D., Department of Geology Reference Collection). As
the properties of the mineral components of the sample depart more
from the norm of the standards, the results become more semi-quanti-
tative. The range of composition and crystallinity of the minerals
in the sample is narrow and does not vary systematically. The intro-
duced error, therefore, is approximately constant. The data has been
used only for comparison within itself, and in this respect is con-
sidered valid.

Niskanen (1964) investigated the accuracy and precision of direct
quantitative x-ray diffraction analysis. The mean error of an analysis
of a synthetic mineral mixture was within two percent. However, the
accuracy of an actual rock analysis was considerably poorer, with a
mean error of approximately ten percent.

The variables affecting the reproducibility of data obtained by
the previously described technique are: (1) inconsistencies in the
measurement of peak intensities; (2) variations in packing the unori-
ented powder and the degree of preferred orientation in the powder;
and (3) variations in the grain size of the powder due to inconsisten-
cies in grinding. To evaluate the affect of these variables on the
reproducibility of the data eight samples were selected and scanned
three times after unloading, remixing, and repacking. The standard
deviations of the computed weight fractions of the individual minerals
in the bulk sample are given in Table 2.

The minimum limit of detectability of a mineral component in the
bulk sample is largely a function of the crystallinity of the substance
(Klug and Alexander, 1954). A poorly crystallized mineral may be a

TABLE 2.   STANDARD DEVIATIONS OF THE WEIGHT FRACTIONS OF MINERALS
OBTAINED BY DIRECT SEMI-QUANTITATIVE X-RAY DIFFRACTION ANALYSIS

Mineral	Standard Deviation (parts per ten)
Quartz	0.08
Potassium Feldspar	0.17
Na-plagioclase	0.34
Analcite	0.10
Muscovite	0.94
Total Clay	0.35

major component of a sample, but may not yield a significant peak.
Generally, a peak was considered significant and the intensity was
measured, if the peak was approximately three standard deviations of
the height of the background peaks above the lower boundary of the
background trace. If a peak did not fulfill the above conditions, but
was still considered present, the minerals was reported as a trace a-
mount. The amount of a mineral that was reported as a trace varies
with the substance. The amount of a mineral reported as undetected
or trace, therefore, may range from complete absence to the maximum
values in Table 3.

Determination of Analcite Composition

Fifteen samples were selected to determine analcite composition.
The samples represent the vertical and lateral extent of analcite-
bearing rocks in the Golden Valley Formation (?). The procedure used
for this analysis was developed by Saha (1959; 1961). It is based on
variation of the (639) peak position of analcite with varying unit cell

TABLE 3.   MINIMUM LEVEL OF DETECTABILITY OF MINERALS BY SEMI-QUANTI-
TATIVE X-RAY DIFFRACTION ANALYSIS

Mineral	Minimum Level of Detectability (parts per ten)
Quartz	0.2
Potassium Feldspar	0.1
Na-plagioclase	0.1
Analcite	0.1
Muscovite	0.2
Total Clay	1.2

composition. The composition is expressed as the silica ratio:

$2\ SiO_2/Na_2O + Al_2O_3$. Silicon was added as an internal standard. The

sample was scanned through 78.5° to 76.0° 2θ at 0.25 degrees per min-

ute, using a chart speed of 15 inches per hour. The previously de-

scribed diffractometer was used. The angular difference between the

(639) peak of analcite and the (331) peak position of silicon was plot-

ted on Saha's (1959) determinative curve, from which the silica ratio

was read. Each sample was scanned three times and an average value was

used. The average of the standard deviations of the replicate analyses

is 0.04.

A predominantly monomineralic specimen (4775) allowed easy con-

centration of analcite for indexing. The sample was crushed and en-

riched by flotation. The decanted fraction, dried, was ground with

a mortar and pestle by hand for ten minutes. Quartz was added as an

internal standard to detect peak shift due to misalignment or instru-

ment response. The sample was scanned through 80° to 2° 2θ at 0.25

degrees per minute, using a chart speed of 15 inches per hour.

Clay Mineral Analysis

Four samples of analcite-bearing arkose were selected for a detailed identification of clay minerals by x-ray diffraction. The samples were disaggregated by crushing and $> 4\phi$ fraction was separated by sieving. Smaller fractions were separated by settling in an aqueous suspension.

Oriented and random mountings were prepared. Oriented mountings of 4μ, 2μ, and $< 1\mu$ fractions were prepared by sedimentation from an aqueous suspension on a glass slide. The suspension was dried at room temperature. Random mountings were prepared of $> 1\mu$ and $< 1\mu$ fractions by passing the sample through a sieve and allowing it to fall on a laquer-coated slide. The oriented samples were treated following Gaudette's (1965) procedure. Samples were heated to 500° C. for one hour and exposed to an ethylene glycol atmosphere for 72 hours. Glycolated and unglycolated pellets were also prepared. A one gram sample of the clay fraction, backed by two grams of cellulose, were compressed in a hydraulic press at eight tons pressure for fifteen seconds.

Randomly mounted specimens were scanned through 38° to 20° 2θ at a rate of 1 degree per minute. Oriented samples were scanned through 50° to 2° 2θ at a rate of 1 degree per minute. The analyses were conducted on the previously described diffractometer. The results of these analyses are discussed on pages 31 and 32.

Grain Size Analysis

Twenty-seven samples representing the lateral and vertical extent of the analcite-bearing arkose were selected for grain size analysis.

The samples were disaggregated by crushing as recommended by Folk (1964). Sand-sized and smaller grains were separated by sieve analysis. The sand-sized grains were divided into the basic divisions of sand-sized material of the Wentworth Scale. The silt-clay fraction was differentiated using North Dakota Geological Survey Procedure A-65 (Clayton, 1965). The results of these analyses are given in Table 8 and Figure 11.

TABLE 4

GENERALIZED SECTION OF FORMATIONS EXPOSED IN THE AREA OF ANALCITE-BEARING SEDIMENTARY ROCKS IN SOUTHWESTERN NORTH DAKOTA

SYSTEM	SERIES	GROUP, FORMATION, MEMBER		MAXIMUM THICKNESS	LITHOLOGIC CHARACTERISTICS	
TERTIARY	MIOCENE	ARIKAREE FORMATION (?)		260 feet (Denson and Gill, 1965)	Greenish-white to light gray cross-bedded sandstone and siltstone interstratified with limestone. Light gray friable sandstones. Pyroclastics. (Denson and Gill, 1965)	
	— UNCONFORMITY —					
	OLIGOCENE	WHITE RIVER GROUP	BRULE FORMATION	250 feet (Denson and Gill, 1965)	Predominantly tuffaceous silts.	
			CHADRON FORMATION	190 feet (Denson and Gill, 1965)	Sandy claystones, coarse-grained locally conglomeratic sandstone, bentonitic claystone, fresh water limestone interbedded with siltstone. (Denson and Gill, 1965)	
	—UNCONFORMITY —					
	EOCENE	GOLDEN VALLEY FORMATION	"DICKINSON" MEMBER	150 feet (Hickey, 1966)	Yellow to gray micaeous sands and sandstones. ?	Massive sandstone up to 70 feet exposed. Tan to white, medium- to coarse-grained. Locally cross-bedded. Questionable western facies of the Golden Valley Formation.
			"HEBRON" MEMBER	45 feet (Hickey, 1966)	Light colored kaolinitic clays and shales (Hickey, 1966) ?	
	UNCONFORMITY					
	PALEOCENE	FORT UNION GROUP	SENTINEL BUTTE FORMATION	620 feet (Royse, 1967a)	Dark gray bentonitic claystone and shale. Buff to brown sandstone. Beds of lignite.	
			TONGUE RIVER FORMATION	520 + feet (Royse, 1967a)	Gray to tan sandstone, siltstone and shale. Beds of lignite.	

described and named by Leonard (1908; 1911). Leonard and Smith (1909) differentiated the Fort Union "Formation" into the Tongue River and Sentinel Butte Members. Royse (1967a) has redefined the Tongue River and Sentinel Butte as formations.

The Tongue River Formation, generally, rests conformably on the Ludlow and Cannonball Formations of the lower Fort Union Group (Denson and Gill, 1965). A local hiatus, however, is recognized at the Tongue River-Cannonball contact (A. Cvancara, Department of Geology, University of North Dakota, personal communication, 1970). The Tongue River Formation is composed of fine- to medium-grained, cross-bedded sandstones, shales, clays, claystones, and lignites. Published measurements of the thickness of the Tongue River Formation vary widely. The author considers Royse's figure for thickness (1967a), of approximately 300 feet in southern Golden Valley County, the most accurate. The Tongue River Formation is exposed in Golden Valley, Billings, Slope, Stark, Dunn, McKenzie, Williams, and Morton Counties, North Dakota (Royse, 1967b).

Sentinel Butte Formation

The Sentinel Butte Formation rests conformably on the Tongue River Formation. It consists of clays, shales, lignites, and sandstones interbedded with sands, siltstones, claystones, and marls. Reports on the thickness of the Sentinel Butte Formation, like the Tongue River Formation, vary widely. The Sentinel Butte Formation is exposed on major buttes in Golden Valley, Billings, and Slope Counties, North Dakota and along the Missouri Escarpment (Royse, 1967b).

TABLE 5   MINERALS IDENTIFIED IN SAMPLES TAKEN IN RECONNAISSANCE STUDY

Specimen*	Quartz	Plagioclase Feldspar	Potassium Feldspar	Analcite	Calcite	Dolomite	Clay	Volcanic Glass	Muscovite
				Sentinel Butte Formation					
5957	X	X					X		X
4749	X	X	X		X		X		
5983	X	X	X				X		X
5997	X	X	X		X	X	X		X
5974	X	X	X	X			X		X
5998	X	X	X		X	X	X		X
5971	X	X	X		X	X	X		
5999	X	X	X		X	X	X		X
6000	X	X	X		X		X		X
6001	X	X	X		X	X	X		X
5984	X		X				X		
6002	X	X	X		X	X	X		X
5985	X		X				X		X

*Refer to Appendix and Figure 1 for areal and stratigraphic positions of cited specimens.

25

TABLE 3 (continued)

Specimen	Quartz	Plagioclase Feldspar	Potassium Feldspar	Analcite	Calcite	Dolomite	Clay	Volcanic Glass	Muscovite
6003	X	X	X	X(?)		X	X		
6004	X	X	X		X	X	X		X
5980	X	X					X		
5978	X	X	X				X		
5986	X						X		

Golden Valley Formation

Specimen	Quartz	Plagioclase Feldspar	Potassium Feldspar	Analcite	Calcite	Dolomite	Clay	Volcanic Glass	Muscovite
4736	X	X	X		X		X		
6005	X	X	X			X	X		X
4724	X	X	X						
4735	X	X	X						
5973	X	X	X						
4739	X	X							
4730	X	X	X						
5989	X	X							

TABLE 3 (continued)

Specimen	Quartz	Plagioclase Feldspar	Potassium Feldspar	Analcite	Calcite	Dolomite	Clay	Volcanic Glass	Muscovite
5981	X	X	X	X			X		X
5982	X	X	X	X			X		X
5975	X	X		X			X		X
5970	X	X	X	X			X		X
5972	X	X	X	X			X		X
5796	X		X	X			X		X

Chadron Formation

Specimen	Quartz	Plagioclase Feldspar	Potassium Feldspar	Analcite	Calcite	Dolomite	Clay	Volcanic Glass	Muscovite
5977	X				X		X		
4694	X	X	X		X		X		

Arikaree Formation (?)

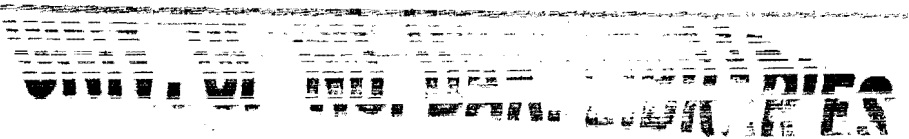| Specimen	Quartz	Plagioclase Feldspar	Potassium Feldspar	Analcite	Calcite	Dolomite	Clay	Volcanic Glass	Muscovite
4742	X	X	X		X	X		X	
4740	X	X	X				X		
4741	X	X	X		X				
5988	X	X	X		X		X		X

27

TABLE 3 (continued)

Specimen	Quartz	Plagioclase Feldspar	Potassium Feldspar	Analcite	Calcite	Dolomite	Clay	Volcanic Glass	Muscovite
5987	X	X	X				X		X
4745	X	X	X		X			X	
4744	X	X	X				X	X	

MINERALS

QUARTZ

Quartz is a constituent of all the analcite-bearing rocks examined. It occurs as anhedral, detrital grains. The grains occur both individually and as composites of individual grains.

The individual grains range in sphericity from 0.3 to 0.5 and average 0.4. The roundness ranges from 0.1 to 0.9 and averages 0.2. The grains have moderate to strong undulatory extinction. They range in diameter from 0.1 mm to 0.3 mm and average 0.2 mm.

The composite quartz grains consist of aggregates of individual grains joined at sutured contacts. The composite grains range in diameter from 0.2 mm to 1.7 mm and average 0.5 mm. The individual grains comprising the aggregates have slight to moderate undulatory extinction, and have approximately the same dimensions as the individual quartz grains described above.

The grains occur in the sediment embedded in the cement or matrix. The grains are commonly embayed (Fig. 2).

FELDSPAR

Detrital plagioclase and potassium are both present in the analcite-bearing arkose. The plagioclase ranges in composition from $Ab_{80}An_{20}$ to $Ab_{55}An_{45}$. However, due to possible ambiguity in determining the sign of extinction angles, the plagioclase may be as albitic as An_{10}. The grains are anhedral and range in diameter from 0.1 mm

29

Figure 2.   Detrital quartz grain. Arrows point out embayed edge.

The quartz grain is embedded in argillaceous matrix.

X 300   Crossed Nicols   Specimen 4670

Figure 3.   Detrital albite grain. Arrow points out pitted edge.

The albite grain is embedded in argillaceous matrix.

X 300   Crossed Nicols   Specimen 4670
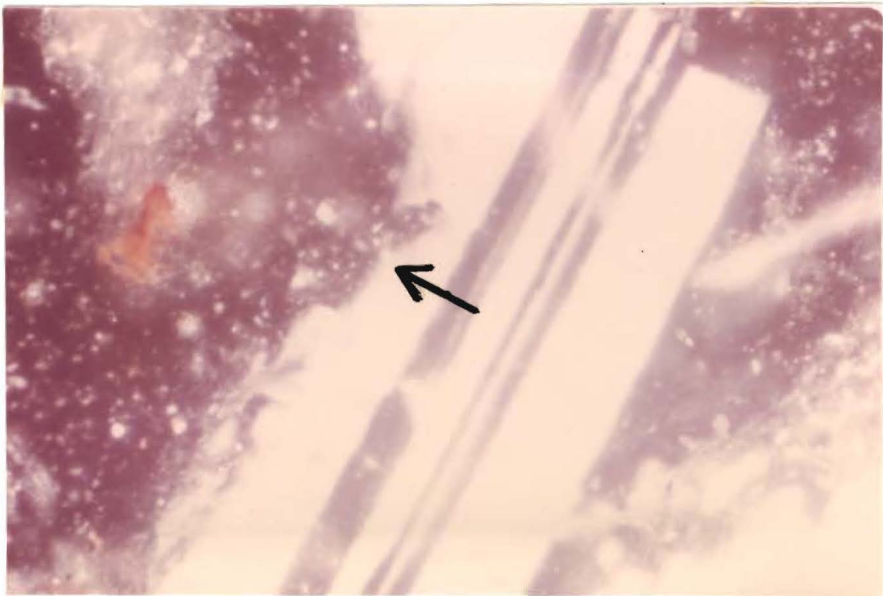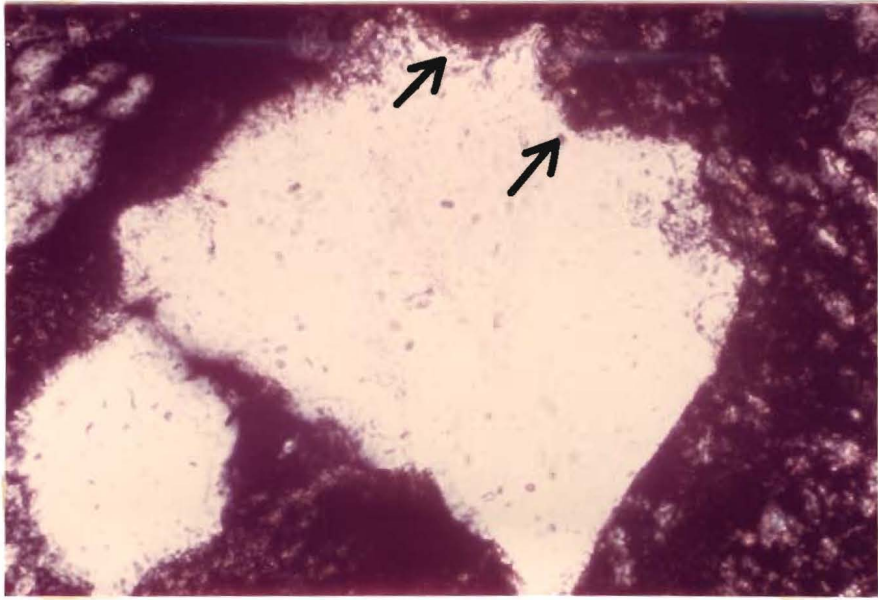
to 1.0 mm and average 0.4 mm. The sphericity ranges from 0.3 to 0.9 and averages 0.6. The roundness ranges from 0.1 to 0.9 and averages 0.3.

The potassium feldspar occurs as microcline and possible orthoclase. The microcline has been identified by the characteristic cross-hatched twinning. The grains identified as orthoclase, however, may be untwinned microcline. The grains range in diameter from 0.1 mm to 1.6 mm and average 0.8 mm. Grain roundness ranges from 0.1 to 0.5 and averages 0.3. The sphericity ranges from 0.5 to 0.9 and averages 0.7.

The detrital feldspars, like the quartz, are commonly embayed (Fig. 3).

CHERT

Detrital chert occurs as anhedral grains ranging in diameter from 0.2 mm to 0.4 mm. There are also isolated and very minor occurrences of spherically shaped, possibly authigenic, chert grains.

ANALCITE

Analcite occurs as spherical and sub-spherical grains ranging in diameter from 0.1 mm to 0.5 mm and averaging 0.2 mm. Three types of grains are recognized: (1) grains with a radial internal structure (Fig. 4); (2) concentrically-structured grains with a massive center and a peripheral radial structure (Fig. 5); and (3) grains without an internal structure or a poorly-defined internal structure (Fig. 6).

This mode of occurrence of analcite fits the definition of the term "spherulite" as used by Pettijohn (1957, p. 96). Spherulites are defined as minute, sub-spherical, radial bodies which have formed in

<u>situ</u>, and which coalesce to form packed polyhedra.

The spherulites with poorly-defined or absent internal structure are the most abundant. Spherulites with radial structure are the next most abundant, followed by the concentrically-structured spherulites.

Analcite is generally thought to be isometric. However, the Maltese cross interference figure on the radial spherulites and the slight birefringence indicates that the analcite is anisotropic. The optical behavior of the spherulites is dependent on the optical properties of the analcite, the state of elastic strain of the individual crystallites, and the relative crystallite orientation. The slight birefringence has been variously attributed to loss of water, strain, or to ordering of the Si, Al atoms in the structure (Deer, <u>et al</u>., 1963). Coombs (1955) has recognized a modification of analcite that is birefringent and biaxial. Departures from the isometric lattice dimensions are not detectable, although weak anomalous reflections may appear.

X-ray diffraction powder data for the Golden Valley (?) analcite (specimen 4775) are given in Table 6. In contrast to the reference data for analcite (ASTM File--7-363, 7-340, and 19-1180) there are a number of minor reflections absent. Most of the absent reflections are in the high angle region ($2\theta > 40°$). In the low angle region ($2\theta < 40°$) three reflections are absent: (411, 330), (420), and (530, 433). This is similar to Crook's (1967) observations, in which the (411, 330), (600, 442), and (200) reflections were noted to be weak or absent. In addition, (721), (811), and (<u>1051</u>) reflections were recognized, but do not correspond to any reflection in the reference data. The significance of these reflections is not immediately apparent. The possibil-

Figure 4.   Analcite spherulite with internal radial structure.
           The internal structure is identified by the Maltese
           cross interference figure.   The partially included
           detrital grain is quartz.   The birefringent rim is
           sericite.   X 600   Crossed Nicols   Specimen 4672

Figure 5.   Analcite spherulite with a massive center and a
           peripheral radial structure.   Dotted line outlines
           the massive center.   The spherulite is embedded in
           a sericitic matrix.   X 600   Crossed Nicols
           Specimen 4672
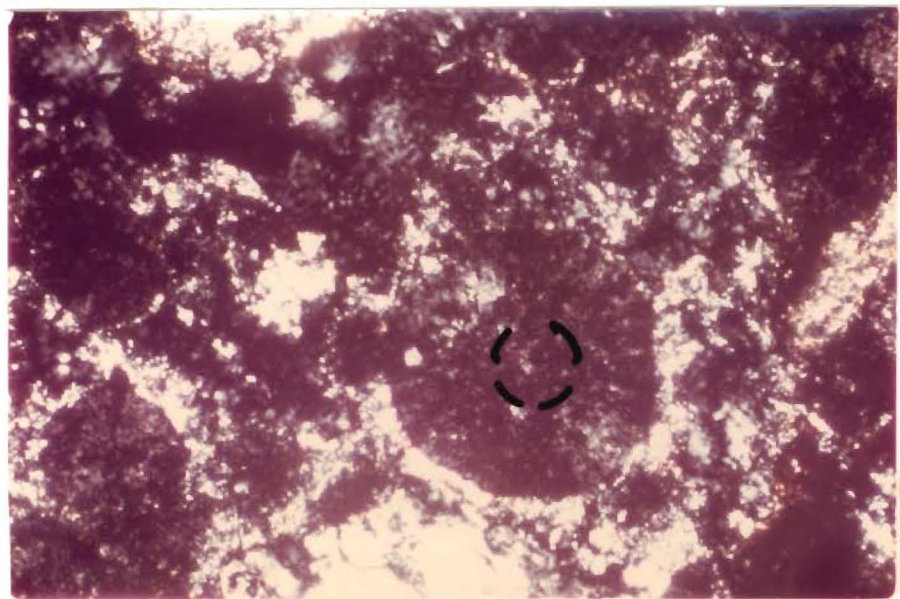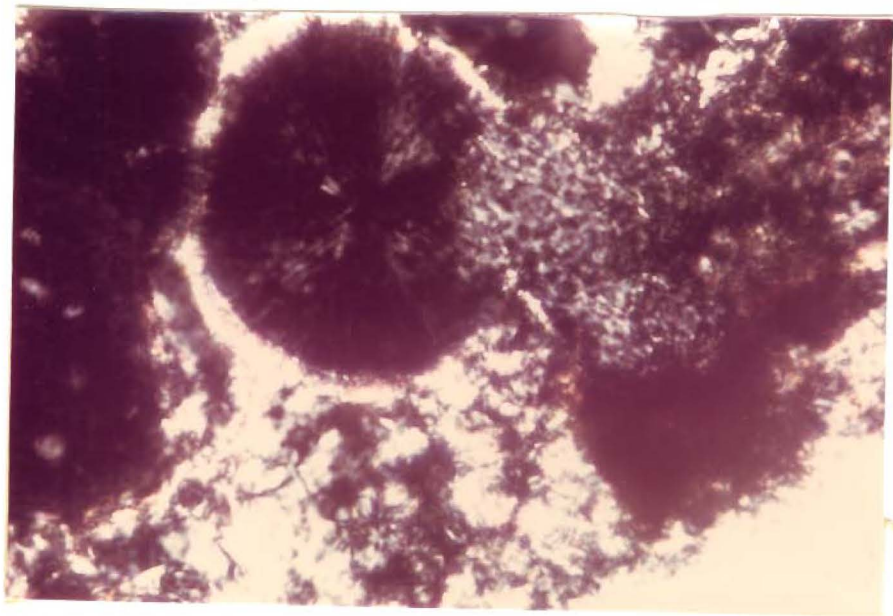
Figure 6.   Distorted, coalesced, analcite spherulites.   These

spherulites do not show any internal structure.

Argillaceous matrix (illite ?) outlines the spherulite

shapes.   X 300   Crossed Nicols   Specimen 4672

Figure 7.   Coarse-grained illitic matrix (sericite).   Black areas

are analcite.   X 600   Crossed Nicols   Specimen 4672
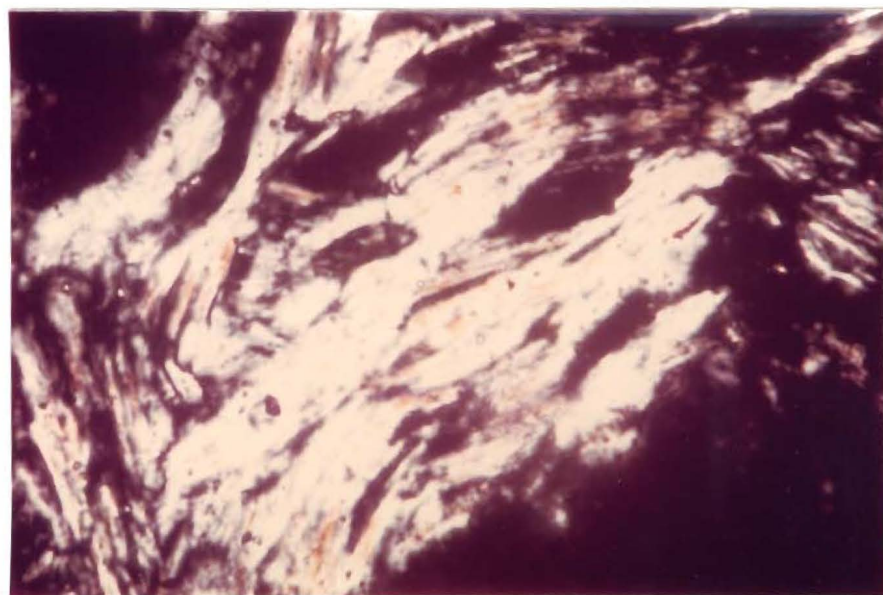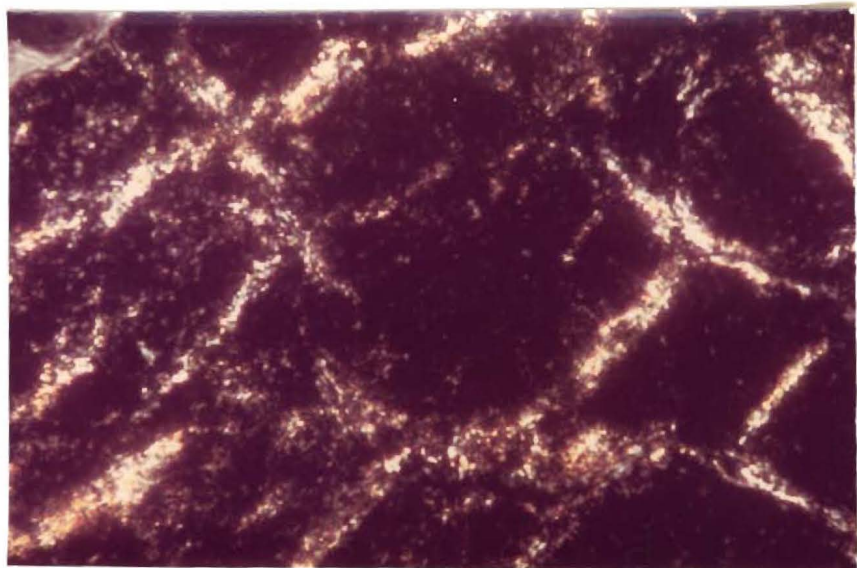
ity of an unrecognized mineral impurity in the sample, however, must be considered.

The composition of analcite is given in Table 7. The extremely fine-grained, polycrystalline nature of the analcite spherulites precluded an accurate determination of the index of refraction.

CLAY MINERALS

Illite, and possibly kaolinite, are the only clay minerals that have been identified in the analcite-bearing rocks. Two textural modifications of the clay minerals have been recognized in thin section. A fine-grained variety occurs in the interstices of the arkose. A coarse-grained variety also occurs in the interstices of the arkose (Fig. 7), and replaces detrital quartz and feldspar. It also occurs as inclusions in the analcite spherulites (Fig. 8). The coarse-grained variety consists of interlocking, platy flakes. This fits the description of authigenic illite outlined by Carrigy and Mellon (1964). The coarse-grained illite replacing quartz also fits the description of authigenic muscovite given by Rex (1966). Coarse-grained illite is generally referred to as sericite (Pettijohn, 1957). Sericite, however, is intermediate in composition between the "ideal" composition of illite and muscovite (Grim, 1968; Reesman and Keller, 1967).

Velde and Hower (1963) have proposed distinguishing between illite polymorphs in sediments as a method for identifying authigenic illite. Attempts to identify the illite polymorphs in various size fractions of the analcite-bearing arkose were not conclusive. The critical peaks for identification of individual polymorphs are very closely spaced (Grim, 1968). The peaks obtained from the samples were broad and dif-

fused, and individual peak positions could not be positively identified.
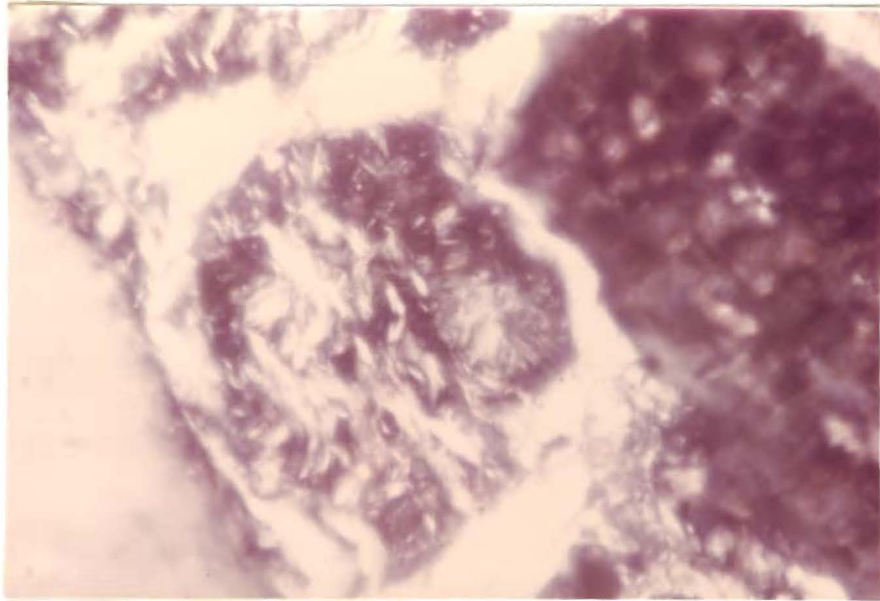
Figure 8.   Sericite inclusions in an analcite spherulite.
             Birefringent rim around spherulite is also sericite.
             Spherulite is adjacent to detrital quartz grain and
             embedded in argillaceous matrix.   X 600   Crossed
             Nicols   Specimen 4672

TABLE 6. X-RAY DIFFRACTION POWDER DATA FOR ANALCITE
(SPECIMEN 4775)

I (obs.)	d (obs.)	d (calc.)	(hkl)
1	6.811	6.860	200
80	5.611	5.600	211
27	4.822	4.852	220
17	3.678	3.667	321
100	3.427	3.430	400
63	2.922	2.925	332
15	2.849	2.801	422
28	2.683	2.691	510, 431
27	2.508	2.505	521
15	2.430	2.425	440
10	2.287	2.287	600, 442
16	2.222	2.256	611, 532
19	1.903	1.903	640
15	1.866	1.867	721
10	1.811	1.802	730
21	1.740	1.748	732, 651
15	1.716	1.715	800
15	1.687	1.689	811
13	1.595	1.595	831
13	1.416	1.400	932, 763
15	1.358	1.294	10̲11
13	1.287	1.288	774
10	1.264	1.265	10̲33
13	1.223	1.220	10̲51

TABLE 7.   COMPOSITION OF ANALCITE

Specimen	2θ Anal. (639)-2θ Si (331)	$2SiO_2/(Na_2O + Al_2O_3)$
4670	$1.80°$	4.28
4775	$1.80°$	4.28
4684	$1.82°$	4.35
4686	$1.80°$	4.28
4678	$1.86°$	4.52
4727	$1.83°$	4.43
6994	$1.76°$	4.00
6995	$1.83°$	4.43
6996	$1.73°$	3.91
7011	$1.91°$	4.85
4778	$1.83°$	4.43
7014	$1.86°$	4.52
4674	$1.82°$	4.35
4773	$1.80°$	4.28
7008	$1.87°$	4.66

ROCK TYPES

ARKOSE

The minerals composing the arkose are quartz, chert, Na-plagio-clase, K-feldspar, analcite, and illite. Chert is a minor constituent and is included as part of the quartz content. Fine-grained illitic matrix and sericite occupy the interstices of the arkose.

The modal composition of the arkose is given in Figure 7. Quartz is generally the most abundant mineral component. Analcite is usually the next most abundant mineral. The average analcite content is approximately 30 percent. The analcite ranges from complete absence to a maximum of approximately 70 percent. The feldspars are relatively minor constituents. The sum of the plagioclase and potassium feldspar contents, on the average, does not exceed more than 20 percent of the composition of the rock. Potassium feldspar is the more abundant variety. Sericite occurs sporadically and is generally a minor component. However, it may comprise as much as 30 percent of the rock.

The classification of the rock as an arkose is based on the amount of feldspar, total clay, and rock fragments present. Metamorphic quartz grains are the rock fragments. These components, re-computed to 100 percent, have been plotted on Folk's (1964) classification diagram (Fig. 10). The majority of the points are in the arkose and subarkose categories.

The arkose is texturally immature and poorly sorted. Grain sized data of the arkose are presented in Table 8. The arkose is character-ized by a relatively high standard deviation. The grain-size mode is

Figure 9. Modal Composition of Analcite-Bearing Arkose

Data from samples cited in Tables 9, 10, 11, and 12.
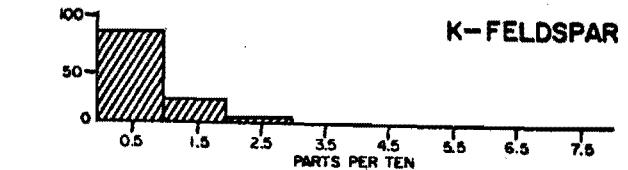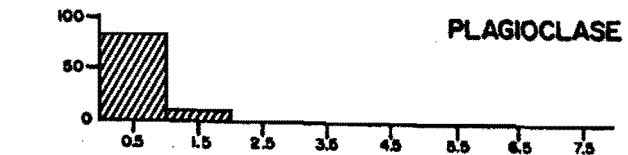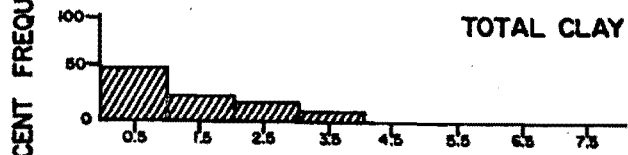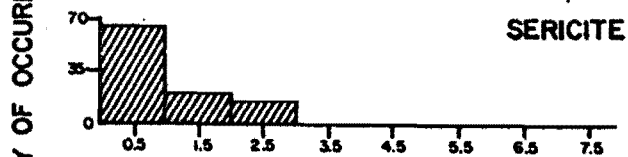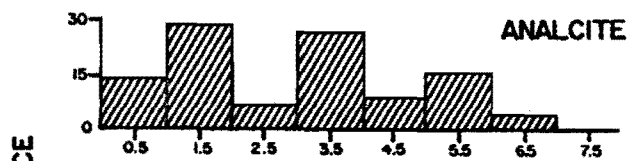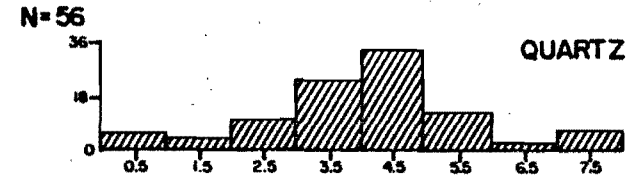
at the very fine sand-coarse silt boundary of the Wentworth size clas-
sification. All samples analyzed show positive skewness toward the fin-
er grain sizes. In a plot of the sand-silt-clay content of the arkose,
the majority of the points fall in the sand corner (Fig. 11). The
grain-size distribution has a narrow range.

· Detrital quartz and feldspar make up the framework of the arkose.
The grains are unoriented in the matrix. A small percentage of the
quartz and feldspar grains are in contact.

The interstices of the arkose are occupied by analcite and illite.
Analcite occurs as individual spherulites in the matrix or as aggregates
of spherulites. In the aggregates the original spherical shape is dis-
torted to a polyhedral shape (Fig. 6). The spherulites range widely
in diameter. Fine-grained illite and coarser sericite frequently out-
line the individual spherulites in the aggregates (Fig. 6). The spher-
ulites range from undistorted individuals in the matrix, to where the
matrix between the spherulites in the aggregates has been reduced to
a veinlet remnant. Matrix may not always be present at the boundaries
of the distorted spherulites.

Analcite and sericite frequently occur together in the arkose.
Sericite often occurs as unoriented inclusions in the spherulites.
Spherulites in the sericite matrix may have indistinct boundaries.
Coarse sericite grains, where in contact with spherulites, are oriented
with their long axes tangential to the spherulites (Fig. 12).

Spherulites occasionally occur in contact with detrital quartz
and feldspar grains and are distorted. The spherulites may partially
or wholly include the detrital grains.

Figure 10.   Mineralogic Classification of Analcite-Bearing Arkose

(After Folk, 1964). Plotted points represent analyzed

samples.
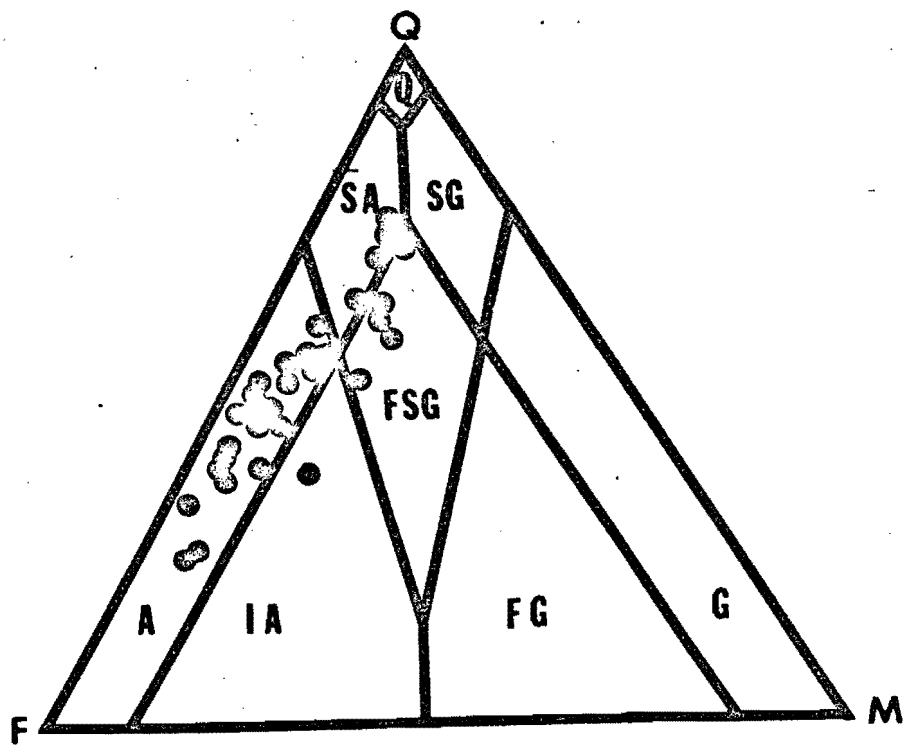
Q-Orthoquartzite
G-Graywacke
A-Arkose
IA-Impure Arkose

SG-Subgraywacke
SA-Subarkose
FSG-Feldspathic
    Subgraywacke
FG-Feldspathic
    Graywacke

TABLE 8

GRAIN SIZE DATA OF ANALCITE-BEARING ARKOSE

Specimen*	Grain Size Median (Q_{50})	Grain Size Mean $M_z=\dfrac{(\emptyset16+\emptyset50+\emptyset84)}{3}$	Skewness $Sk_I=\dfrac{\emptyset16+\emptyset84-2\emptyset50}{2(\emptyset84-\emptyset16)}+\dfrac{\emptyset5+\emptyset95-2\emptyset50}{2(\emptyset95-\emptyset5)}$	Standard Deviation $\sigma_I=\dfrac{\emptyset84-\emptyset16}{4}+\dfrac{\emptyset95-\emptyset5}{6.6}$
4708	3.6 $\emptyset$	4.3 $\emptyset$	+ 0.56	1.3 $\emptyset$
4691	3.3 $\emptyset$	3.9 $\emptyset$	+ 0.65	1.8 $\emptyset$
4783	3.1 $\emptyset$	3.3 $\emptyset$	+ 0.57	1.3 $\emptyset$
4788	3.5 $\emptyset$	3.9 $\emptyset$	+ 0.63	1.2 $\emptyset$
4748	3.1 $\emptyset$	3.5 $\emptyset$	+ 1.43	1.3 $\emptyset$
4774	3.5 $\emptyset$	4.0 $\emptyset$	+ 0.82	1.7 $\emptyset$
4747	3.5 $\emptyset$	3.9 $\emptyset$	+ 0.45	1.4 $\emptyset$
4785	3.3 $\emptyset$	3.9 $\emptyset$	+ 0.64	1.6 $\emptyset$
4680	3.2 $\emptyset$	3.7 $\emptyset$	+ 0.61	1.3 $\emptyset$
4675	3.0 $\emptyset$	3.5 $\emptyset$	+ 0.71	1.5 $\emptyset$
4776	3.1 $\emptyset$	3.5 $\emptyset$	+ 0.64	1.3 $\emptyset$
4686	3.1 $\emptyset$	4.6 $\emptyset$	+ 1.33	1.5 $\emptyset$
4672	3.6 $\emptyset$	4.2 $\emptyset$	+ 0.53	1.8 $\emptyset$
4783	3.3 $\emptyset$	3.7 $\emptyset$	+ 0.46	1.5 $\emptyset$

*Refer to Appendix and Figure 1 for stratigraphic and areal locations of cited specimens

TABLE 8 (continued)

Specimen	Grain Size Median (Q_{50})	Grain Size Mean $M_z=\dfrac{(\phi16+\phi50+\phi84)}{3}$	Skewness $Sk_I=\dfrac{\phi16+\phi84-2\phi50}{2(\phi84-\phi16)}+\dfrac{\phi5+\phi95-2\phi50}{2(\phi95-\phi5)}$	Standard Deviation $\sigma_I=\dfrac{\phi84-\phi16}{4}+\dfrac{\phi95-\phi5}{6.6}$
4670	3.4 φ	4.0 φ	+ 0.57	1.6 φ
4671	3.5 φ	4.1 φ	+ 0.55	1.5 φ
4679	3.2 φ	4.0 φ	+ 1.21	1.0 φ
4687	3.1 φ	3.6 φ	+ 0.66	1.3 φ
4673	3.1 φ	3.6 φ	+ 0.66	1.8 φ
4674	3.2 φ	3.5 φ	+ 0.50	1.3 φ
4689	3.1 φ	3.4 φ	+ 0.51	1.1 φ
4688	3.0 φ	3.3 φ	+ 0.71	1.1 φ
4707	3.4 φ	4.0 φ	+ 0.58	1.6 φ
4787	3.4 φ	4.1 φ	+ 0.62	1.8 φ

Figure 11.   Grain-Size Distribution of Analcite-Bearing Arkose

Plotted points represent analyzed samples.

clay (> 8.00)

sand
(1.00—4.00)

silt
(4.00—8.00)
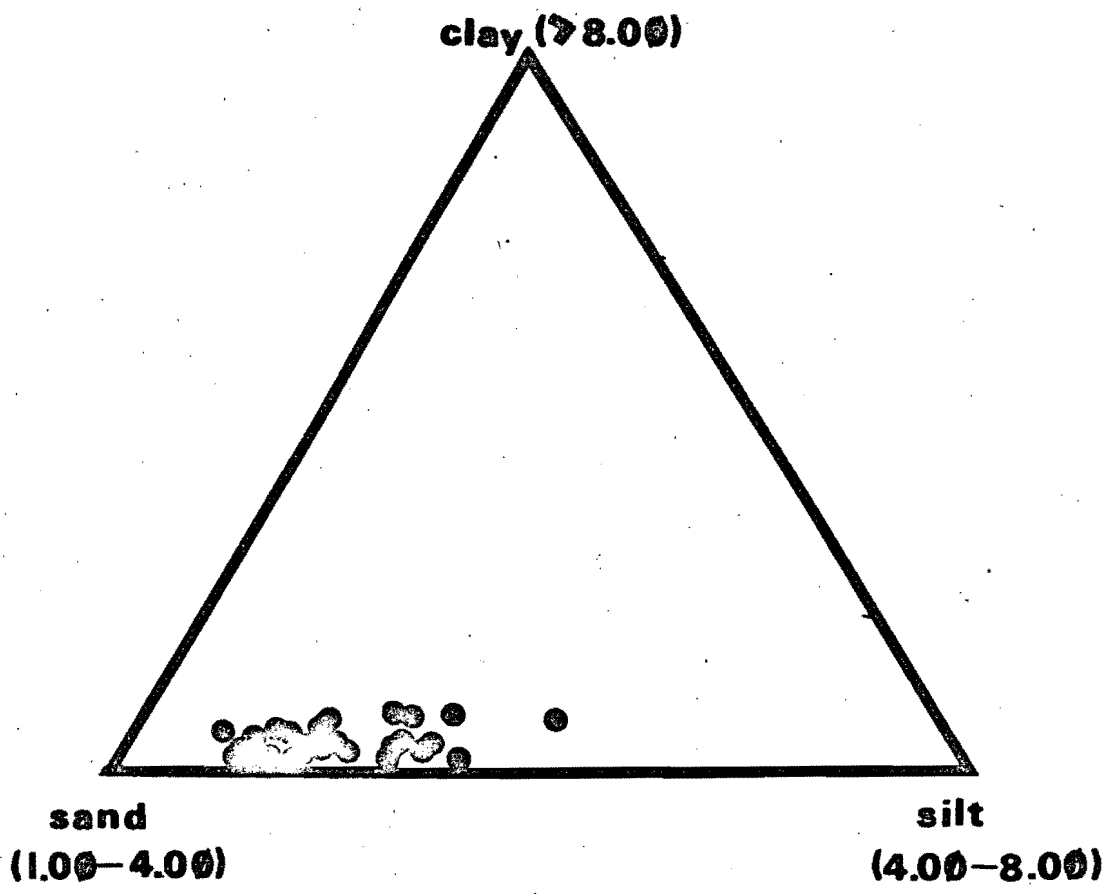
There are some differences in analcite content of the arkose in its lateral extent. The modal compositions of the arkose from the different buttes are given in Tables 9, 10, 11, and 12. Arkoses from Slide and Chalky Buttes have the lowest average analcite content, approximately 15 percent. Arkoses from Sentinel and Flat Top Buttes have approximately the same average analcite contents, 30 percent. Arkose from Bullion Butte has the highest average analcite content, approximately 40 percent.

The analcite-bearing arkose, compared to the modal compositions of "typical" arkoses (Pettijohn, 1957), is notably deficient in potassium and plagioclase feldspars.

ANALCIMOLITE

The minerals composing the analcimolite are analcite, quartz, and illite. Analcite is consistently the predominant mineral component. The term analcimolite is applied to a rock type in which analcite is the principle mineral constituent. The analcite content ranges from approximately 40 percent to 80 percent and averages approximately 60 percent. The modal composition of the analcimolite is given in Figure 14.

Quartz grains form the framework of the analcimolite. The grains have high sphericity and low roundness, and have an average diameter of 0.17 mm. Analcite does not occur as spherulites as it does in the arkose, but occupies the interstices of the analcimolite as the cementing material. Analcite in the analcimolite appears to be massive, but a red stain outlines what might be individual grains (Fig. 13).

Figure 14. Modal Composition of Analcimolite.

Data from samples cited in Tables 11 and 12.

ANALCITE

QUARTZ

TOTAL CLAY

PERCENT FREQUENCY OF OCCURRENCE

PARTS PER TEN
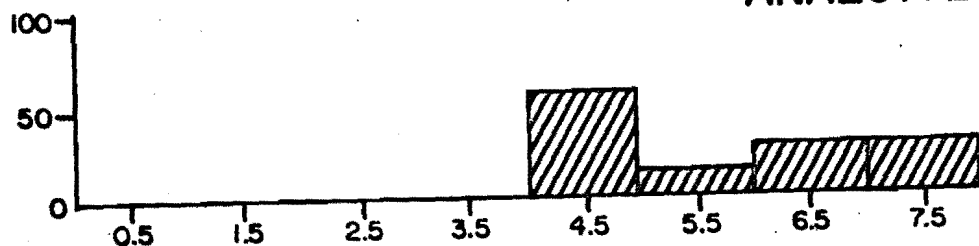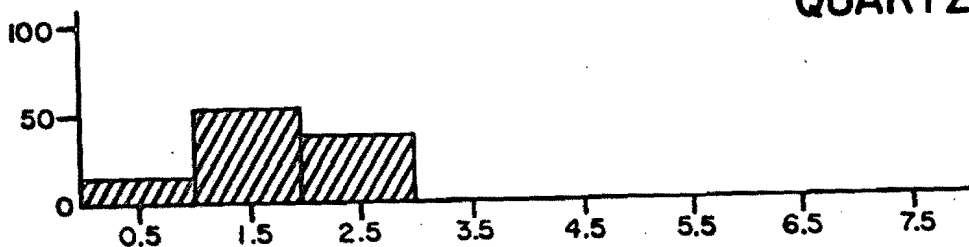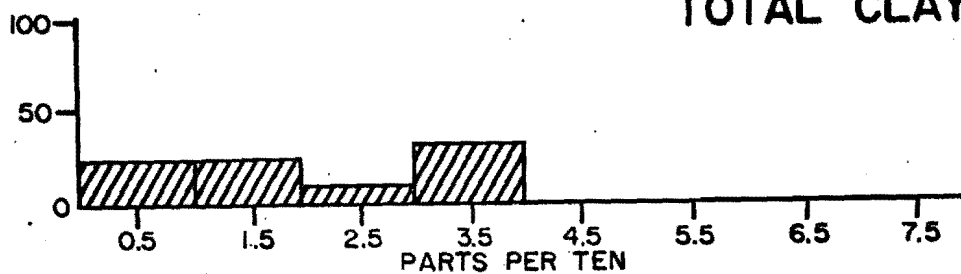
The average diameter of these possible grains is 0.08 mm. Analcite composing the analcimolite has approximately the same composition as analcite in the arkose. Illite is present as irregular masses in the analcite.

There is some variation in the analcite content of the analcimolite in its lateral extent. Analcimolite from Slide Butte has the highest average analcite content, approximately 70 percent. Analcimolite from Chalky Buttes has the lowest average analcite content, approximately 50 percent. Analcimolite from Bullion Butte has an average analcite content of approximately 60 percent. The modal compositions of the analcimolite from the different buttes are given in Tables 11 and 12.

Figure 12. Coarse sericite flakes oriented tangential to the
periphery of spherulites. Black area area analcite
spherulites.   X 600   Crossed Nicols   Specimen 4670

Figure 13. Texture of Analcimolite.   X 150   Parallel Light
Specimen 4775
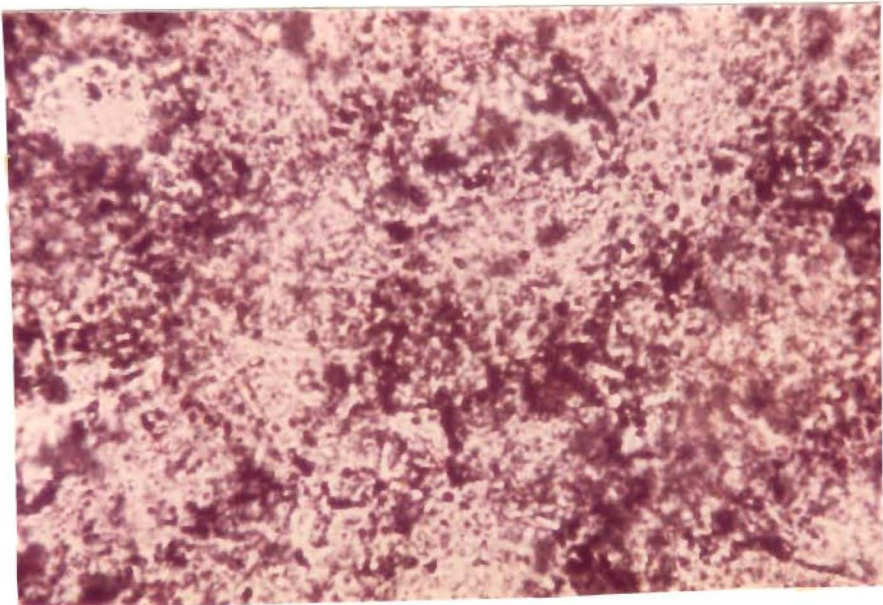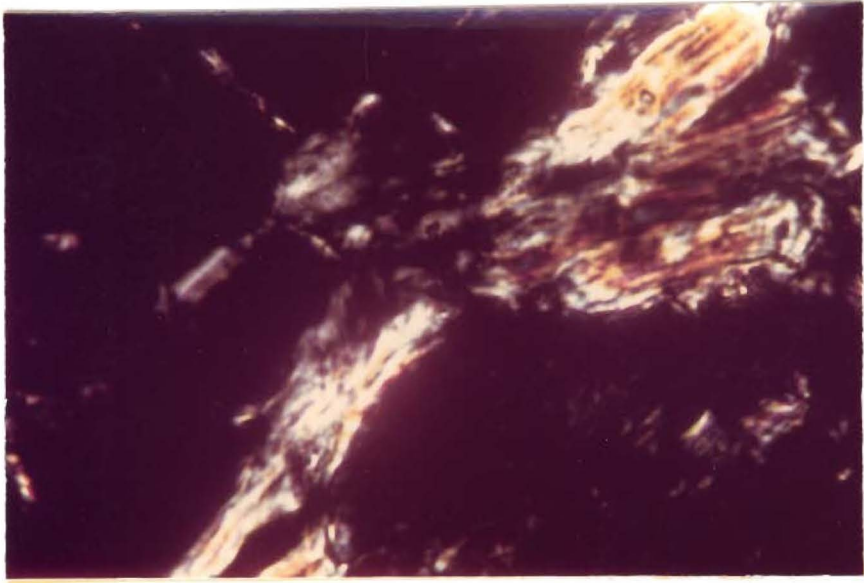
TABLE 9

MODAL COMPOSITION OF ANALCITE-BEARING ROCKS ON SENTINEL BUTTE
T. 139 N., R. 104W., GOLDEN VALLEY COUNTY

Specimen*	Quartz	Plagioclase	K-Feldspar	Analcite	Muscovite (sericite)	Total Clay	Total
7008	4.6**	-	0.7	5.9	-***	T****	11.2
7009	3.8	0.6	0.4	1.2	-	3.0	9.0
7010	4.8	-	0.4	3.7	-	T	8.9
7011	3.4	1.5	0.7	1.8	-	2.0	9.4
7012	5.6	1.0	0.7	0.7	2.0	1.5	11.5
4708	4.2	-	1.3	5.3	T	2.5	13.3
4705	4.4	1.5	0.6	3.9	1.3	T	11.7
4681	4.6	T	0.9	3.4	-	T	8.9
4690	3.8	0.4	0.6	2.0	-	3.0	9.8
4680	1.4	0.4	0.9	3.2	T	2.5	8.4
5970	4.2	T	0.8	3.3	1.6	T	9.9
4675	4.6	0.9	2.1	2.6	2.7	T	12.9
7013	3.4	-	0.6	5.6	-	T	9.6

*Refer to Appendix and Figure 1 for stratigraphic and areal locations of cited specimens.
**Mineral contents expressed as parts per ten
***Mineral not detected
****Mineral detected only in trace amount

59

TABLE 9 (con't.)

Specimen	Quartz	Plagioclase	K-Feldspar	Analcite	Muscovite (sericite)	Total Clay	Total
5981	3.2	0.8	0.7	1.7	3.1	T	9.5
4689	2.7	1.3	1.2	2.0	-	2.5	9.7
4693	4.4	1.0	1.0	1.3	T	2.0	9.7
4682	4.7	T	1.2	4.7	T	T	10.6
4686	3.4	T	0.9	3.9	T	2.0	10.2
4707	3.4	o.4	0.9	1.7	T	2.5	8.9
4679	3.8	0.4	1.7	3.7	-	T	9.6
4688	4.9	1.0	0.9	2.1	T	2.0	10.9
7014	5.3	T	0.7	4.2	1.3	T	11.3
7015	3.9	0.4	0.5	1.9	2.6	2.0	11.3

60

TABLE 10

MODAL COMPOSITION OF ANALCITE-BEARING ROCKS ON FLAT TOP BUTTE
T. 139 N., R. 104 W., GOLDEN VALLEY COUNTY

Specimen	Quartz	Plagioclase	K-Feldspar	Analcite	Muscovite (sericite)	Total Clay	Total
4785	2.6	2.6	0.5	1.6	-	4.0	9.3
4672	5.9	T	0.4	4.0	1.3	T	11.6
4669	4.3	1.0	1.6	-	-	2.5	9.4
4674	5.1	T	-	6.2	1.5	T	12.8
4787	4.2	-	1.5	-	-	4.0	10.0
4670	3.3	T	0.7	3.9	-	2.0	0.9
4788	3.1	-	0.5	4.3	-	2.0	9.9
4673	5.7	T	-	3.7	T	1.5	10.9
4671	4.4	T	0.9	3.6	T	2.0	10.9
4748	4.6	0.8	0.9	-	1.6	2.0	9.9
4747	3.8	T	0.5	3.3	3.1	2.0	9.7

TABLE 11

MODAL COMPOSITION OF ANALCITE-BEARING ROCKS ON BULLION BUTTE
T. 137 N., R. 102 W., BILLINGS COUNTY

Specimen	Quartz	Plagioclase	K-Feldspar	Analcite	Muscovite (sericite)	Total Clay	Total
4779	0.8	-	-	5.9	-	3.1	9.8
4770	2.7	-	-	5.9	T	2.0	10.6
4783	2.5	1.2	1.4	1.4	-	2.5	9.0
4775	1.0	-	-	6.2	-	2.0	9.2
7007	1.9	-	-	6.6	-	1.0	9.5
4771	5.1	1.0	0.5	0.5	-	2.0	9.1
4774	5.9	T	0.9	3.3	2.2	1.0	13.3
4782	4.4	T	-	4.2	1.3	T	9.9
7016	5.0	T	T	5.0	T	T	10.0
4773	0.9	-	-	5.3	-	3.0	8.2
4684	5.0	T	-	5.4	1.3	-	11.7
4785	4.2	-	-	6.0	-	-	10.2
4777	7.0	-	-	2.0	2.6	-	11.6
4772	2.4	0.6	1.7	3.2	-	2.0	9.9

TABLE 12

MODAL COMPOSITION OF ANALCITE-BEARING ROCKS ON SLIDE AND CHALKY BUTTES
T. 139 N., R. 101 W., SLOPE COUNTY

Specimen	Quartz	Plagioclase	K-Feldspar	Analcite	Muscovite (sericite)	Total Clay	Total
6994	2.2	--	--	6.3	--	T	8.5
6998	8.0	0.4	0.7	3.9	--	--	11.0
6999	7.6	0.4	0.3	1.4	T	T	9.7
6997	4.4	1.3	0.5	1.6	T	2.0	9.8
7000	7.2	0.4	0.3	1.1	--	T	9.0
7001	3.6	T	1.0	2.0	T	4.0	10.6
7002	2.5	--	--	7.3	--	T	9.8
6995	1.9	--	--	4.9	--	3.0	9.8
7003	2.1	--	--	4.7	--	3.0	9.9
7004	7.2	1.3	0.9	0.7	1.3	1.5	12.8
7005	1.7	1.3	0.8	1.1	--	4.0	8.9
4729	7.7	--	0.5	1.1	--	2.0	11.3
4727	2.0	--	--	6.0	1.3	1.5	9.0
6996	1.5	--	--	7.7	--	T	9.2
7006	2.1	--	--	4.6	--	2.0	8.7

63

DISCUSSION

MINERAL ASSOCIATIONS

The association and significance of the following materials, with respect to the occurrence of analcite, will be dealt with in turn: volcanic glass, quartz, plagioclase, potassium feldspar, and sericite.

Analcite-Pyroclastic Association

Pyroclastic materials containing volcanic glass are in close proximity to the analcite-bearing rocks of the Golden Valley Formation (?). Ash beds are present above and below the analcite-bearing rocks on Sentinel, Flat Top, and Chalky Buttes.

The recognized genetic relationship between analcite and volcanic glass warrants consideration of the tuffaceous material as precursor to the analcite. A survey of the occurrences of analcite believed to have originated from pyroclastic materials shows that the vitroclastic texture is commonly preserved (Bradley, 1928; 1929; Bramlette and Posnjak, 1933; Ross, 1941; Coombs, 1954; Deffeyes, 1959; Gulbrandsen and Cressman, 1960; Brown and Thayer, 1963; Terrugi, 1964; Loughnan, 1966; Ijima and Utada, 1966; Robinson, 1966; Wilkinson and Whetten, 1967). This texture is not present in the arkose of analcimolite, suggesting that the analcite in these occurrences has not been derived from volcanic glass.

Whetten and Coombs (1967) have proposed a genetic classification of sedimentary analcites based on composition. Analcites originating from siliceous volcanic glasses are silica-rich. The Si/Al ratio of

2θ Anal.(639)-Si(331)	Inferred Composition (anhydrous)	Group A	Group B	Group C	Golden Valley (?) Analcite
2.13	$Na_{12}Al_{12}Si_{36}O_{96}$				
.12					
2.10					
.09					
.08					
.07					
.06					
.05					
.04					
.03	$Na_{13}Al_{13}Si_{35}O_{96}$				
.02					
.01					
2.00					
.99					
.98					
.97					
.96					
.95					
.94	$Na_{14}Al_{14}Si_{34}O_{96}$				
.93					
.92					
.91					Ar
1.90					
.89					
.88					
.87					Ar
.86					Ar, Ar
.85	$Na_{15}Al_{15}Si_{33}O_{96}$				
.84					
.83					Ar, Ar, An
.82					Ar, Ar
.81					
1.80					Ar, Ar, Ar, An
.79					
.78					
.77	$Na_{16}Al_{16}Si_{32}O_{96}$				
.76					An
.75					
.74					
.73					An
.72					
.71					
1.70					

Explanation

Group A--Silica-rich analcites formed from siliceous volcanic glass by
   inferred reaction with saline waters.

Group B--Analcites occurring in a burial metamorphic environment.

Group C--Silica-poor analcites inferred to be formed by direct precipi-
   tation or by reaction of highly alkaline water with sediment.

Ar--Composition of analcite in arkose; An--Composition of analcite in
   analcimolite.

Figure 15.   Classification of Analcite Based on Composition (After
           Whetten and Coombs, 1967)

the Golden Valley (?) analcite is low, 2.0 to 2.4. Analcite of this
low Si/Al composition is generally considered to have originated by
direct precipitation from highly alkaline waters, or by reaction of
such waters with clay minerals or other sedimentary materials (Fig.
15).

Analcite-Quartz Association

Detrital quartz is present in all of the analcite-bearing rocks
examined. There is no apparent relationship in the distribution of
quartz and analcite in the analcite-bearing rocks. The detrital
quartz in the analcite-bearing rocks is embayed. The embayments are
interpreted as the effects of dissolution by reaction with interstitial
water. There is no textural indication of analcite replacing the
quartz.

The majority of natural, fresh, surface waters are undersaturated
with respect to amorphous silica, but supersaturated with respect to
quartz. However, the corroded condition of the quartz suggests that
a solution in contact with the sediment, at some time in the history
of the sediment, was undersaturated with respect to quartz.

Analcite-Feldspar Association

There is a well-defined relationship in the distribution of anal-
cite and the detrital feldspars. A plot of analcite versus plagioclase
contents of the analcite-bearing arkose shows a decrease in plagioclase
with an increase in analcite (Fig. 16). Curves have been calculated
by the method of least squares for the point distributions in Figures

Figure 16.   Scatter Diagram of Analcite-Detrital Plagioclase
Data taken from specimens cited in Tables 9, 10, 11, and
12.

Y=3.9X^{-0.5513}

r=0.62

PLAGIOCLASE (Parts per ten)

ANALCITE (Parts per ten)
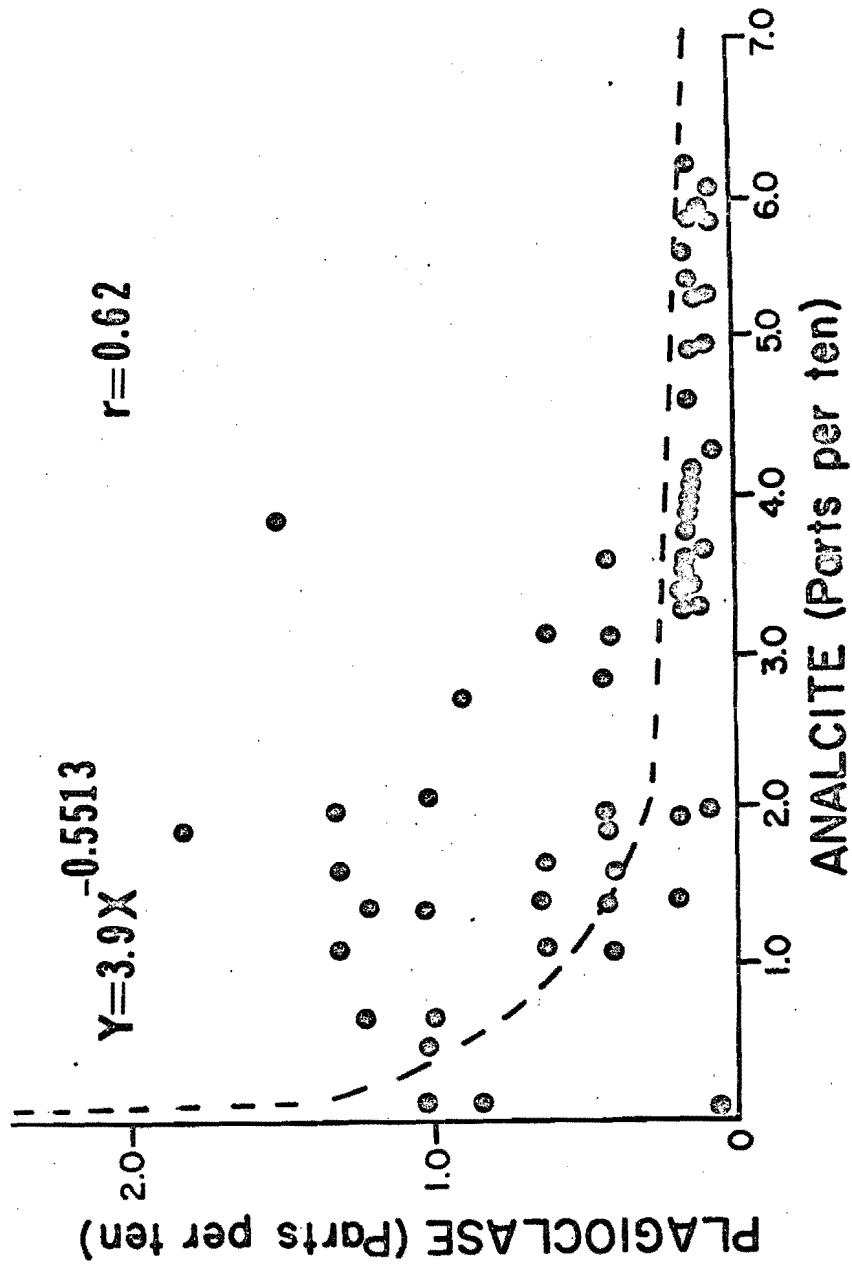
Figure 17.   Scatter Diagram of Analcite-Detrital Potassium Feldspar
Data taken from specimens cited in Tables 9, 10, 11, and
12.
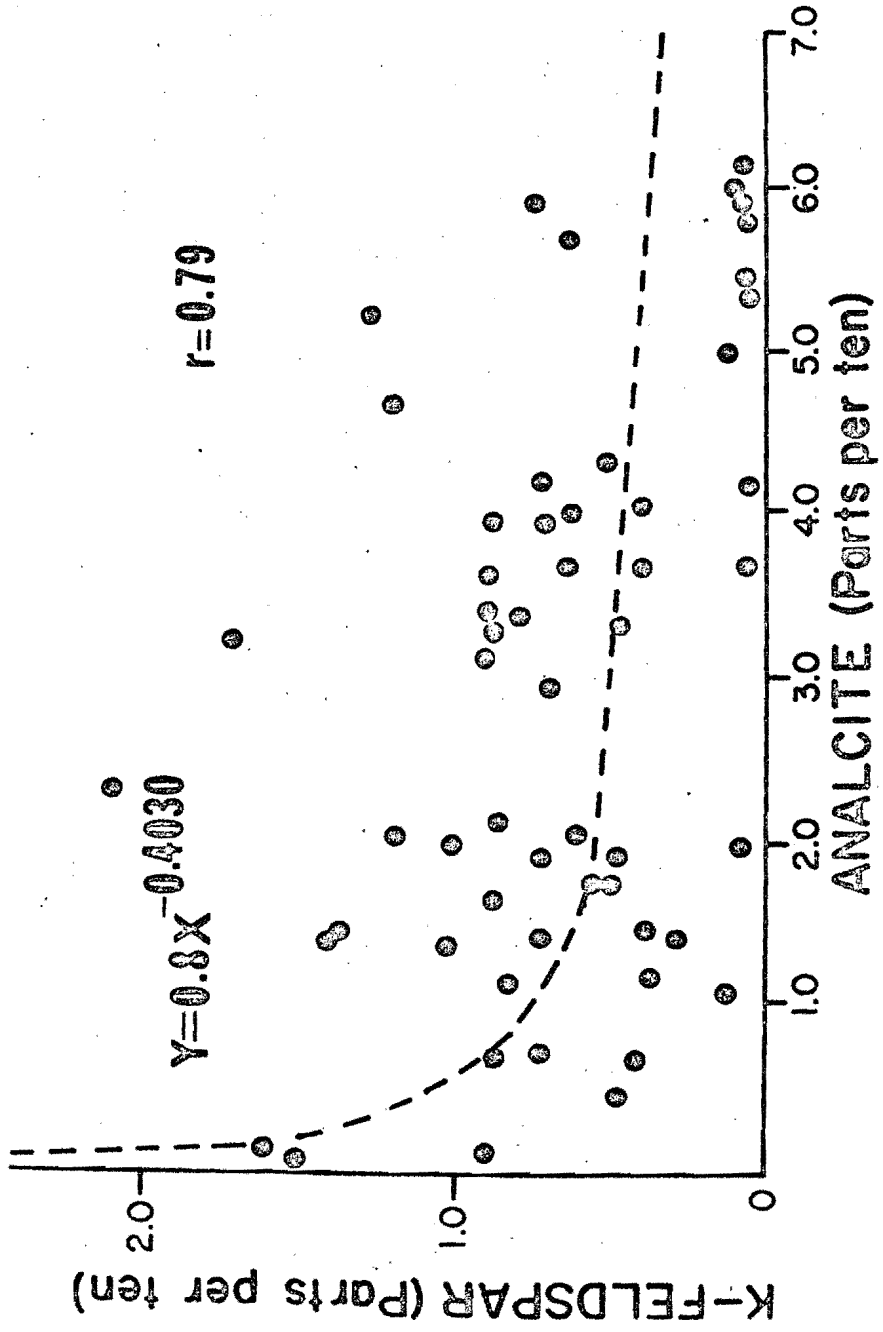
K-FELDSPAR (Parts per ten)

ANALCITE (Parts per ten)

$Y=0.8X^{-0.4030}$

$r=0.79$

16, 17, and 18. The curves are the best possible fits for the trends of the point distributions and give the highest correlation coefficients. The calculated curve in Figure 18 defines the point distribution as curvilinear. The curve is used only to define qualitatively the point distribution. There is a similar curvilinear relationship

16, 17, and 18. The curves are the best possible fits for the trends of the point distributions and give the highest correlation coefficients. The calculated curve in Figure 18 defines the point distribution as curvilinear. The curve is used only to define qualitatively the point distribution. There is a similar curvilinear relationship between analcite and potassium feldspar (Fig. 17).

The curvilinear distribution of the previously described relationship can be explained by the vertical distribution of analcite, plagioclase, and potassium feldspar in the section (Fig. 21). The analcite content increases upward in the section. Correspondingly, the feldspar content decreases upward in the section. The significance of the vertical distribution of these minerals has been statistically tested. The unit has been divided into a lower 30 foot section and an upper 30 foot section. The statistical significance of the differences between the mean mineral contents of the upper and lower halves of the section have been computed. Table 13 gives the confidence levels at which differences in the mean mineral contents in the upper

TABLE 13.---Confidence Levels at which the Hypothesis $\overline{X}_{>30} \neq \overline{X}_{<30}$ can be accepted as Significant

Mineral	$\overline{X}_{>30}$	$\overline{X}_{<30}$	Confidence Level
Analcite	4.3 ppt.	2.3 ppt.	99.5 %
Plagioclase	0.2 ppt.	0.5 ppt.	99.5 %
K-Feldspar	0.7 ppt.	0.8 ppt.	70 %

and lower halves of the section can be accepted as significant. The calculated regression curves show the vertical distribution of the

minerals to also be curvilinear.

It is concluded, from the distribution relationships, that anal-
cite has been derived from the detrital feldspars. This conclusion
is supported by the results of mineral synthesis experiments, in
which analcite has been produced in reactions between albite and water
(Friedman, 1951; Fredrickson and Cox, 1954; Morey and Chen, 1955; Sand,
Roy, and Osborn, 1957; Morey and Fournier, 1961). Textural relation-
ships in the arkose indicate that analcite is not directly replacing
the feldspars. The analcite occurs as distinct spherulites. There
is no penetration or embayment of the feldspars by analcite.

The equilibrium conditions for the reaction between analcite and
albite have been experimentally investigated. Campbell and Fyfe (1965)
determined the temperature and pressure of equilibrium for the reaction:

$$NaAlSi_2O_6 \cdot H_2O + SiO_2 \rightleftharpoons NaAlSi_3O_8 + H_2O$$
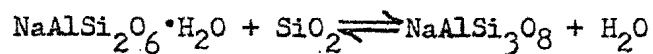
At conditions of low P_{H_2O} the reaction is at equilibrium at approxi-
mately 190° C. At temperatures less than 190° C. analcite is stable
relative to albite.

Silica activity can displace the equilibrium temperature (Camp-
bell and Fyfe, 1965). The corroded condition of the detrital quartz
and feldspar suggests that the silica activity of the solution may be
a significant factor in controlling the analcite-feldspar relation-
ship. If a solution is saturated with respect to amorphous silica,
the dissolution of albite will be depressed (Fyfe and McKay, 1962).
Under such conditions albite would be stable relative to analcite at
temperatures less than 190° C. The corroded quartz, however, suggests

Figure 18. Vertical Distribution of Analcite, Plagioclase, and Potassium Feldspar. Data taken from specimens cited in Tables 9, 10, 11, and 12.
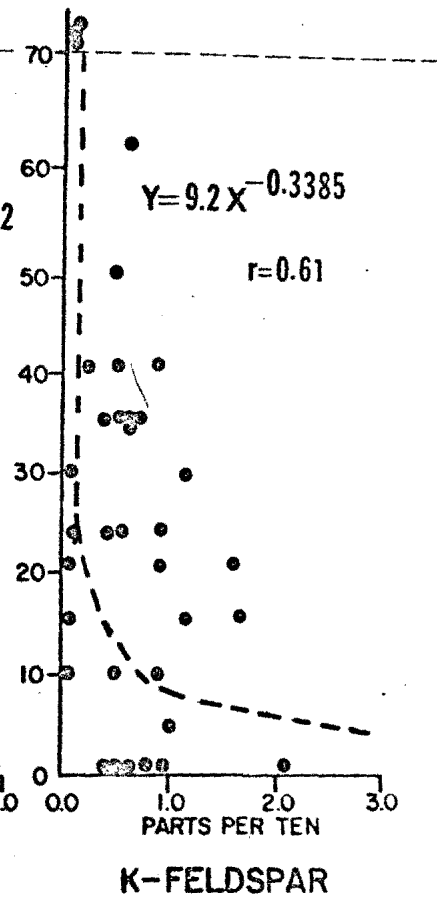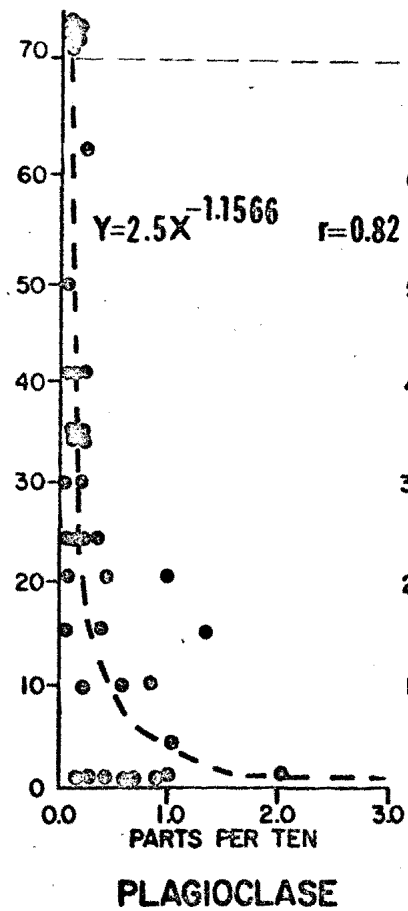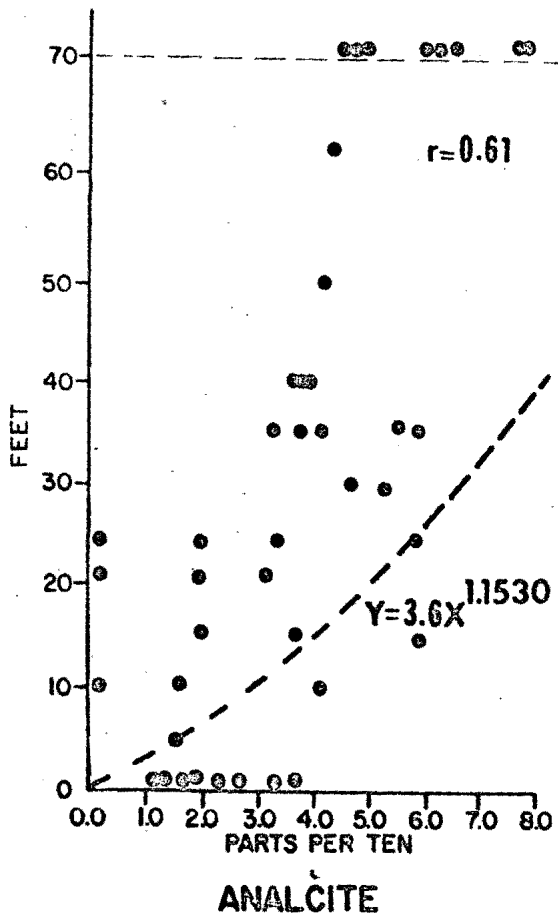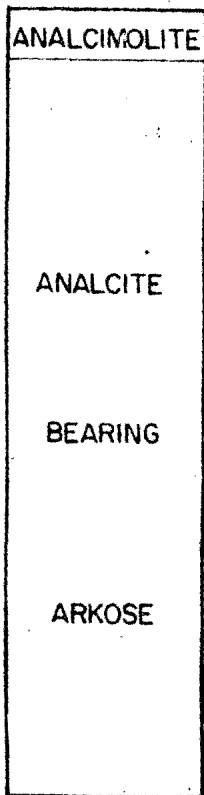
that the solution was undersaturated with respect to quartz. Consequently, the albite was probably easily dissolved in the solution.

Hess (1966) has approximated the fields of stability of minerals in the system $Na_2O-K_2O-Al_2O_3-SiO_2-H_2O$ at 25° C., on the basis of the composition of the solution in equilibrium with the minerals (Fig. 19). The single hachured area in Figure 19 represents the composition of natural lake and river waters (data from Livingstone, 1963). The surface water compositions are outside the stability field of analcite. The double hachured area is the composition of a solution in contact with analcite (Hay and Moiola, 1963). This solution is assumed to be in equilibrium with analcite, and representative of a solution from which analcite would crystallize. The arrow is a crude, hypothetical, approximation of the change in composition of fresh surface water to produce a solution from which analcite would crystallize. The origin of the arrow has been purposely placed to the left of the

$- \text{Log} \left[SiO_2 \right] = 4$ isopleth, the solubility of quartz. The corroded condition of the detrital quartz, as previously discussed, suggests that the original solution was undersaturated with respect to quartz. The proposed solution from which analcite would crystallize, as inferred from Hess's (1967) diagram, was undersaturated with respect to silica, alkaline, and had a high Na^+ concentration. It has been pointed out that solutions of this composition usually do not exist at the surface of the earth. However, after burial the reaction of interstitial water with the mineral components of the sediment, in the relatively closed system that would be produced by burial, could easily establish solutions of the required concentration. As the quartz and

Figure 19. Isoplethic section at $\log \frac{K^+}{H^+} = 4$ of phase diagram for the system $Na_2O-K_2O-Al_2O_3-SiO_2-H_2O$ (after Hess, 1966). Single hachured symbol represents range in composition of lake and river waters. Double hachured symbol represents the composition of a solution in equilibrium with analcite. See text for discussion.
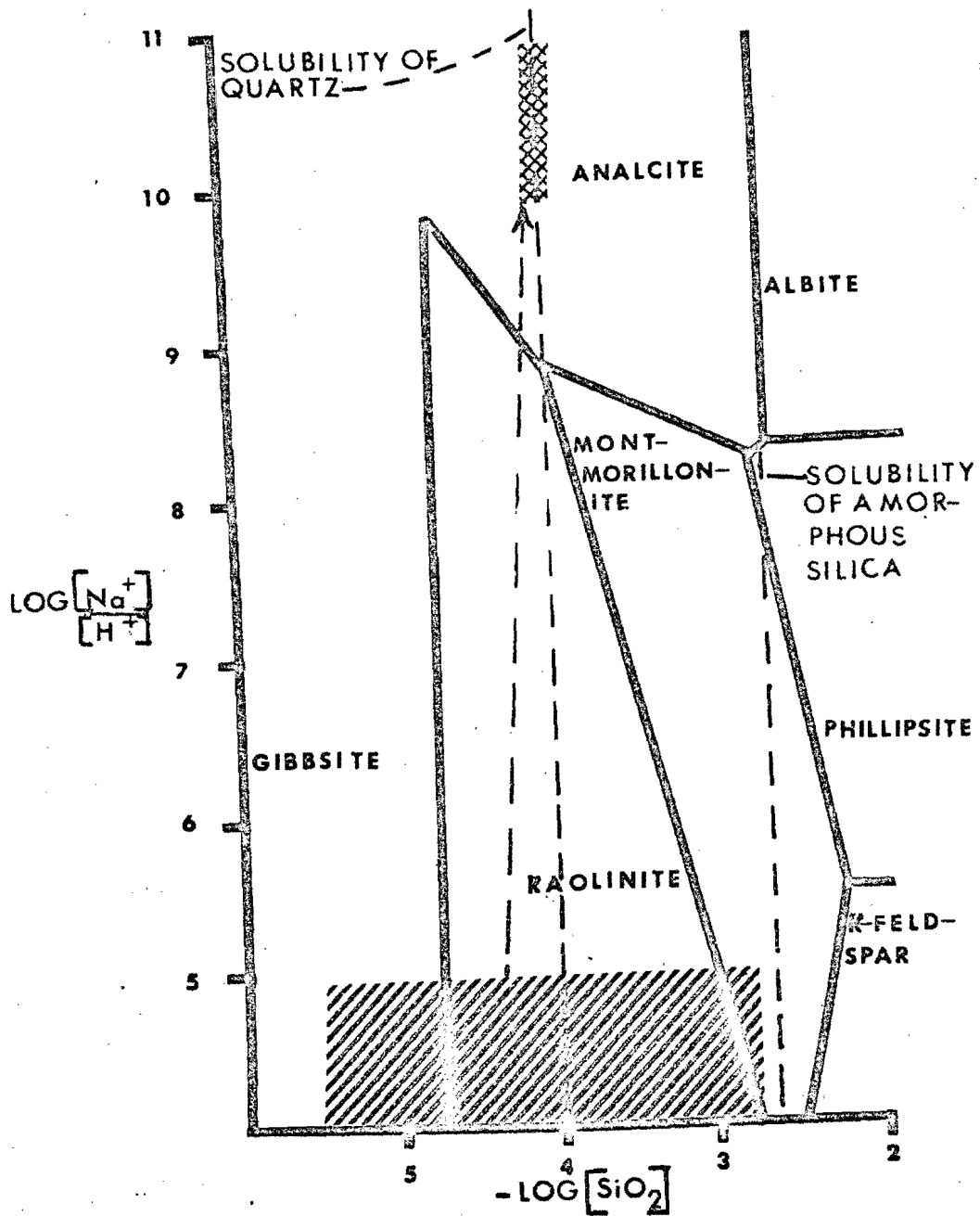
feldspars dissolved, the solution composition moved to the right with increasing silica concentration. The composition would also move upward, as indicated by the arrow, since the dissolved feldspars would add to the cation concentration and increase the pH of the solution. The pH, however, would be maintained at moderate alkalinity. As the silica concentration of the solution increased due to dissolution of the quartz and feldspars, the solubility of the feldspars would be depressed. Thus, the silica acts as a buffer. The potassium feldspar probably reacted similarly, except that it is less soluble than sodium plagioclase (Keller, et al., 1963). According to Hess's (1967) scheme, therefore, when the solution reaches a critical concentration of $[Na^+]$, $[H^+]$, and $[SiO_2]$, analcite would crystallize.

This reasoning is supported by data presented by Harris (1967), in which it has been shown that pore waters in a contemporary fluvial sediment have a higher silica concentration than the overlying surface water.

This approximation of an environment that would crystallize analcite has been inferred from the relative distributions of the minerals, and the condition of the coexisting minerals. There are undoubtedly other governing factors. However, their influence is not immediately apparent or they cannot be evaluated by only a study of the natural mineral occurrences. Some of these probable factors are the influence of the groundwater recharge system, the biological activity, and the interdependence among the various dissolution-precipitation reactions.

It is therefore proposed that analcite crystallized from interstitial solutions in the rock, from constituents derived from the dis-

solving feldspars. The dissolution and precipitation reactions
probably took place at a relatively shallow depth of burial. The
texture of the arkose suggests that it did not undergo extensive com-
paction. A very small percentage of the coarse clastic grains forming
the framework of the arkose are in contact. Most of the compaction
probably took place in the argillaceous matrix.

The vertical distribution of analcite and feldspar in the unit
is attributed to the removal of the interstitial water, the reaction
media, with increasing depth of burial. Thus, the dissolution of the
feldspars was impeded, halting the reaction sequence.

Analcite-Sericite Association

Sericite occurs in the arkose as a matrix surrounding the analcite
and as unoriented inclusions in the analcite spherulites. The textural
relationship suggests that the sericite formed prior to the analcite,
or at least prior to the formation of the spherulites. The oriented,
coarse sericite grains at the periphery of the spherulites suggest
that they have been pushed aside as the spherulites grew. Some of
the sericitic matrix was probably included by the spherulites as they
formed.

The possible significance of the analcite-sericite association in
the arkose, is that sericite has been produced, along with analcite,
in minerals synthesis reactions between albite and water (Morey and
Chen, 1955; Morey and Fournier, 1961). Sericite, like analcite, crys-
tallizes from alkaline solutions (Hemley, 1959). Thus, sericite and
analcite may be products of the same environment and an interdependent

reaction.

FORMATION OF SPHERULITES

Spherulitic crystallization has been recognized in igneous, meta-morphic, and sedimentary rocks. Three origins for spherulitic struc-tures are proposed: (1) crystallization from a colloid; (2) segrega-tion of disseminated mineral matter; and (3) crystallization from supersaturated, high polymer solutions. The applicability of these origins to the analcite spherulites are considered.

Spherically-shaped bodies are generally thought to have crystal-lized from a colloid (Rust, 1935). However, the textural criteria that has been generally interpreted as characteristic of colloidal crystal-lization has been critically reviewed (Roedder, 1968). It has been demonstrated that the textural features, colloform shape, syneresis cracks, concentric banding, and radial structures, do not necessarily result from colloidal crystallization.

The textural relationships among the individual spherulites also suggest that they did not crystallize from a colloid. Colloids have high water contents and crystallization involves dessication and con-traction. The mutual interference and distortion of the spherulites suggests expansion and coalescence. The orientation of the coarse sericite grains to the periphery of the spherulites also suggests an increase in volume. As the spherulites grew they pushed the sericite grains aside, orienting them. It is concluded, on the basis of these considerations, that the spherulites did not crystallize directly from

a colloid.

A colloidal phase, however, may possibly have been an intermediate stage. Experimental studies (Fredrickson and Cox, 1954) on the solubility of albite produced a gel from which analcite crystallized. The analcite, however, crystallized as a single crystal and not as a spherulite.

Pettijohn (1957) and Ramberg (1958) attribute the development of accretionary forms, such as spherulites, to differentiation. It is proposed that mineral assemblages are most stable when segregated. This is based on the assumption that the rock mass will have a lower free energy, and will therefore be more stable, if the mineral is segregated rather than disseminated. This explanation adequately accounts for the occurrence of the spherulites. It has not, however, been experimentally verified.

Spherulitic crystallization from a supersaturated, high-polymer solution has been theoretically considered (Sears, 1963) and experimentally investigated (Bassett, et al., 1963; Magill, 1965). Spherulites are recognized to be the usual mode of crystallization of high polymers (Sears, 1961).

The formation of a spherulite, rather than a single crystal, is a function of the critical radius of nucleation (Sears, 1961). There has been little investigation of the nucleation and polymerization of silicates in solution. Consequently, there is little basis for evaluation of the conditions which might crystallize spherulites or single crystals. The type of spherulitic structure that develops from a spherulitic nucleus is determined by the conditions under which growth, as

distinct from nucleation, occurs (Sears, 1961; Magill, 1965). The observed differences in the analcite spherulite structures, therefore, may be due to changes in conditions during growth (eg. solution concentration, temperature).

Microscopic examination has revealed only limited information that could be used to infer the origin of the spherulites. Modifications in the spherulite structures suggests that there may have been some differences in the conditions governing spherulite growth, or that the spherulites may have undergone varying degrees of recrystallization after formation. Observed textural relationships indicate that direct crystallization of the spherulites from a colloid is unlikely. However, there is little basis to distinguish between differentiation or crystallization from a supersaturated, high-polymer solution as possible origins for the spherulites.

RELATIONSHIP OF ANALCITE OCCURRENCES IN THE ARKOSE AND ANALCIMOLITE

The compositions of nalacite in the arkose and analcimolite vary within a narrow range (Fig. 20). Analcite in the arkose is slightly more siliceous than analcite in the analcimolite. The average composition of analcite in the arkose is 4.39. The average composition of analcite in the analcimolite is 4.08.

The composition of analcite in sedimentary rocks is a function of the parent material from which it has been derived, and the composition of the solution from which it crystallized (Whetten and Coombs, 1967; Ijima and Hay, 1968). The analcite in the arkose and analcimo-

lite are silica-poor (see Fig. 15).

Analcite in the arkose and analcimolite have different textural appearances. Analcite in the arkose occurs as spherulites and in the analcimolite it occurs as a matrix devoid of structure. The analcimolite has a smaller detrital mineral fraction than the arkose.

The analcimolite rests on the analcite-bearing arkose. The analcite content of the arkose increases upward in the section. The analcimolite appears to be a culmination of the increasing analcite content of the unit (see Fig. 14). It has been demonstrated that analcite in the arkose has been derived from the detrital feldspars. However, there is no evidence to warrant extending this relationship to the analcimolite. The contact between the arkose and the analcimolite is sharp. There is no indication of interaction between the two rock types.

On the basis of compositional similarities between analcite in the arkose and the analcimolite, it is concluded that they came from similar parent materials (see Fig. 15; Explanation; Group C). Proposed origins for analcimolite-like rocks that appear applicable to the Golden Valley (?) analcimolite are by direct precipitation from solution (Van Houten, 1962) and by crystallization of gels from alkaline springs (Eugster and Jones, 1968). There is no evidence to indicate that the formation of analcite in the arkose and analcimolite was either dependent or independent.
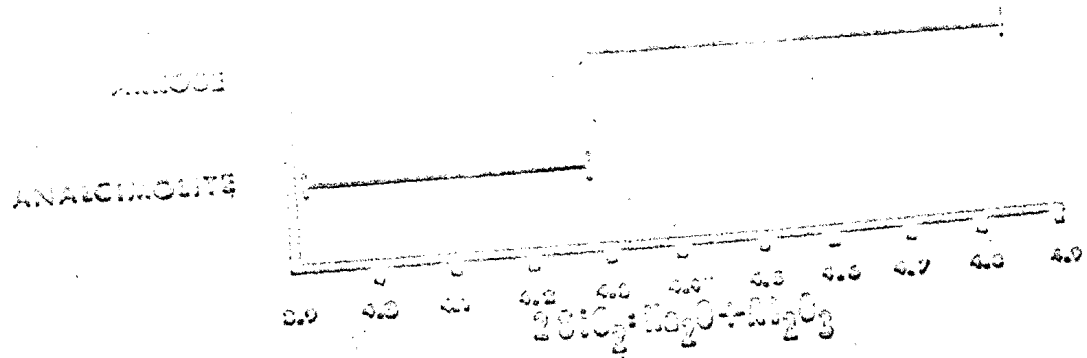
Figure 20. COMPARISON OF COMPOSITION RANGE OF ANALCITE IN THE ARKOSE AND ANALCIMOLITE

RELATIONSHIP OF ANALCITE DISTRIBUTION TO THE POST-EOCENE UNCONFORMITY

Denson (written communication to W.J. Stone, 1970) has defined the regional distribution of analcite: "In our experience, the occurrence of analcite is restricted <u>largely</u> to the rocks directly underlying the regional unconformity at the base of the Oligocene and Miocene. In the Williston Basin analcite can and does occur in all formations transected by this unconformity." The tentativeness of this observation is stressed, since the mineralogy of the rocks in the Tertiary sequence has not been completely examined in detail. The Tertiary rocks in which analcite does appear are the arkose and analcimolite assigned to the Golden Valley Formation and the sands of the Sentinal Butte and Tongue River Formations.

The significance of the restriction of analcite to rocks below the post-Eocene unconformity is not immediately apparent. The absence of analcite in these rocks may reflect climatic changes or differences in the mineral composition and physical properties (eg. porosity, permeability) of the sediment. These possibilities, however, are speculative, and should be considered as largely tentative until there has been a more detailed examination of the mineralogy of the rocks above the post-Eocene unconformity, to determine the validity of Denson's observation.

SUMMARY OF CONCLUSIONS

1. Analcite occurs in two distinct rock types, arkose and analcimo-
   lite. Analcite constitutes up to about 60 percent of the arkose
   and up to 80 percent of the analcimolite.

2. The analcite-bearing rocks are possibly late Eocene in age, and
   have been tentatively included in the Golden Valley Formation.

3. The analcite occurs in the arkose as spherulites. Three types
   of spherulites are recognized: (1) spherulites with a radial in-
   ternal structure; (2) spherulites with a massive center and a
   peripheral radial structure; and (3) spherulites with no internal
   structure, or a poorly-defined internal structure. Proposed origins
   for the spherulites are by diagenetic differentiation or by crystal-
   lization from a supersaturated, high polymer solution. The anal-
   cite is least abundant at the base of the arkose unit, and increas-
   es upward. The abundances of the analcite and the detrital feld-
   spars are inversely related. It is proposed that analcite in the
   arkose crystallized from alkaline, interstitial solutions, under-
   saturated with respect to silica and with high Na^+ concentration.
   The required constituents were derived from feldspars dissolving
   in the interstitial solutions. Sericite occurs with the analcite
   in the arkose as a possible associated alteration product.

4. Analcite occurs in the analcimolite as a cement. Proposed origins
   for the analcimolite are by precipitation from surface waters, or
   by crystallization of gels from alkaline springs.

86

5. Analcite in the arkose and analcimolite is silica-poor. Analcite in the arkose, however, is more siliceous than analcite in the analcimolite.

APPENDIX

APPENDIX

AREAL LOCATIONS AND STRATIGRAPHIC POSITIONS OF SPECIMENS CITED IN TEXT
(Numbered Localities Refer to Figure 1)

Specimen	Areal Location	Stratigraphic Position	Lithology
		SENTINEL BUTTE FORMATION	
5971	T. 139 N., R. 104 W., sec. 6, se. 1/4, sw. 1/4, Golden Valley County.	Southwest side of Sentinel Butte; Base of white bed, 40 feet below Sentinel Butte-Golden Valley contact; locality 5.	Clayey sand
5979	T. 139 N., R. 104 W., sec. 6, se. 1/4, sw. 1/4, Golden Valley County.	Southwest side of Sentinel Butte; base of white bed, 40 feet below Sentinel Butte-Golden Valley contact; locality 5.	Sandy clay
5984	T. 139 N., R. 104 W., sec. 6, se. 1/4, sw. 1/4, Golden Valley County.	Southwest side of Sentinel Butte; 9 feet above base of White Bed, approximately 40 feet below Sentinel Butte-Golden Valley contact; locality 5.	Clay and claystone
5985	T. 139 N., R. 104 W., sec. 6, se. 1/4, sw 1/4, Golden Valley County.	Southwest side of Sentinel Butte; top of White Bed, approximately 40 feet below Sentinel Butte-Golden Valley contact; locality 5.	Clay
6004	T. 139 N., R. 104 W., sec. 6, se. 1/4, sw. 1/4, Golden Valley County.	Southwest side of Sentinel Butte; 40 feet below Golden Valley-Sentinel Butte contact; locality 5.	Lignite

Specimen	Areal Location	Stratigraphic Position	Lithology
5974	T. 139 N., R. 104 W., sec. 6, ne. 1/4, nw. 1/4, Golden Valley County.	Southwest side of Sentinel Butte; 30 feet below Golden Valley-Sentinel contact; locality 5.	Sandstone
6005	T. 139 N., R. 104 W., sec. 6, sw. 1/4, se. 1/4, Golden Valley County.	Southwest side of Sentinel Butte; 10 feet below Golden Valley-Sentinel Butte contact; locality 5.	Unconsolidated sand
5986	T. 139 N., R. 104 W., sec. 6, sw. 1/4, se. 1/4, se. 1/4, Golden Valley County.	Southwest side of Sentinel Butte; 6 feet below Golden Valley-Sentinel Butte contact; locality 5.	Silty clay
5998	T. 139 N., R. 104 W., sec. 8, ne. 1/4, sw. 1/4, Golden Valley County.	Northwest side of Flat Top Butte; 45 feet below Sentinel Butte-Golden Valley contact; base of white bed; locality 10.	Clay
5999	T. 139 N., R. 103 W., sec 3, nw. 1/4, nw. 1/4, Golden Valley County.	Northeast side of Sentinel Butte; 100 feet below summit of butte; locality 3.	Sandstone
6001	T. 139 N., R. 104 W., sec. 8, ne. 1/4, sw. 1/4, Golden Valley County.	Northwest side of Flat Top Butte; 40 feet above top of white bed; locality 10.	Unconsolidated sand
5978	T. 139 N., R. 104 W., sec. 6, se. 1/4, nw. 1/4, Golden Valley County.	North of Sentinel Butte; 100 feet below Golden Valley-Sentinel Butte contact; locality 23.	Mudstone
5980	T. 139 N., R. 103 W., sec. 3, nw. 1/4, ne. 1/4, Golden Valley County.	Approximately one-half mile east of Sentinel Butte; exact stratigraphic position not determinable; locality 9.	Mudstone

Specimen	Areal Location	Stratigraphic Position	Lithology
6003	T. 139 N., R. 103 W., sec. 17, ne. 1/4, sw. 1/4, Golden Valley County.	Southwest side of Flat Top Butte; exact stratigraphic position not determinable; locality 13.	Clay
5983	T. 139 N., R. 104 W., sec. 8, ne. 1/4, sw. 1/4, Golden Valley County.	Northwest side of Flat Top Butte; 60 feet above top of white bed; locality 10.	Unconsolidated sand

GOLDEN VALLEY FORMATION (?)

Specimen	Areal Location	Stratigraphic Position	Lithology
5997	T. 139 N., R. 96 W., sec. 1, nw. 1/4, sw. 1/4, Stark County.	East side of Dobson's Butte; 5 feet below summit of butte; locality 21.	Sandstone
4735	T. 138 N., R. 96 W., sec. 1, ne. 1/4, sw. 1/4, Stark County.	South side of small butte; 16 feet below summit of butte; locality 22.	Silica-cemented sandstone
4736	T. 138 N., R. 96 W., sec. 20, sw. 1/4, ne. 1/4, Stark County.	East side of small butte; summit of butte; locality 20.	Sandstone
4730	T. 138 N., R. 96 W., sec. 20, sw. 1/4, ne. 1/4, Stark County.	Northwest side of minor butte; summit of butte; locality 22.	Silica-cemented sandstone
5989	T. 138 N., R. 96 W., sec. 20, sw. 1/4, ne. 1/4, Stark County.	Northwest side of minor butte: 2 feet below summit of butte; locality 22.	Silica-cemented sandstone

Specimen	Areal Location	Stratigraphic Position	Lithology
4724	T. 138 N., R. 96 W., sec. 20, ne. 1/4, sw. 1/4, Stark County.	South side of minor butte; base of butte; locality 22.	Silica-cemented sandstone
5973	T. 138 N., R. 96 W., sec. 7, ne. 1/4, sw. 1/4, Stark County.	East side of minor butte; summit of butte; locality 19.	Silica-cemented sandstone
4735	T. 138 N., R. 96 W., sec. 7, ne. 1/4, sw. 1/4, Stark County.	East side of minor butte; 3 feet below summit of butte; locality 19.	Silica-cemented sandstone
4729	T. 134 N., R. 101 W., sec. 28, nw. 1/4, sw. 1/4, Slope County.	Northeast side of Slide Butte; summit of butte; location 17.	arkose
4734	T. 134 N., R. 101 W., sec. 28, nw. 1/4, sw. 1/4, Slope County.	Northeast side of Slide Butte; summit of butte; location 17.	arkose
7002	T. 134 N., R. 101 W., sec. 28, nw. 1/4, sw. 1/4, Slope County.	South side of Slide Butte; summit of butte; locality 26.	analcimolite
6994	T. 134 N., R. 101 W., sec. 28, nw. 1/4, sw. 1/4, Slope County.	South side of Slide Butte; summit of butte; locality 26.	analcimolite
4727	T. 135 N., R. 101 W., sec. 28, nw. 1/4, sw. 1/4, Slope County.	Northeast side of Slide Butte; 7 feet below summit of butte; locality 17.	arkose
7004	T. 134 N., R. 101 W., sec. 15, ne. 1/4, ne. 1/4, Slope County.	North end of Chalky Buttes; 40 feet below Golden Valley-Chadron contact; locality 18.	arkose

Specimen	Areal Location	Stratigraphic Position	Lithology
6998	T. 134 N., R. 101 W., sec. 15, ne. 1/4, ne. 1/4, Slope County.	North end of Chalky Buttes; 35 feet below Golden Valley- Chadron contact; locality 18.	arkose
6997	T. 134 N., R. 101 W., sec. 15, ne. 1/4, ne. 1/4, Slope County.	North end of Chalky Buttes; 30 feet below Golden Valley- Chadron contact; locality 18.	Arkose
6999	T. 134 N., R. 101 W., sec. 15, ne. 1/4, ne. 1/4, Slope County.	North end of Chalky Buttes; 30 feet below Golden Valley- Chadron contact; locality 18.	Arkose
7000	T. 134 N., R. 101 W., sec. 15, ne. 1/4, ne. 1/4, Slope County.	North end of Chalky Buttes; 30 feet below Golden Valley- Chadron contact; locality 18.	Arkose
7001	T. 134 N., R. 101 W., sec. 15, ne. 1/4, ne. 1/4, Slope County.	North end of Chalky Buttes; 25 feet below Golden Valley- Chadron contact; locality 18.	Silty claystone
7006	T. 134 N., R. 101 W., sec. 15, ne. 1/4, ne. 1/4, Slope County.	North end of Chalky Buttes; 19 feet below Golden Valley- Chadron contact; locality 18.	Analcimolite
6996	T. 134 N., R. 101 W., sec. 15, ne. 1/4, ne. 1/4, Slope County.	North end of Chalky Buttes; 19 feet below Golden Valley- Chadron contact; locality 18.	Analcimolite
7005	T. 134 N., R. 101 W., sec. 15, ne. 1/4, ne. 1/4, Slope County.	North end of Chalky Buttes: 16 feet below Golden Valley- Chadron contact; locality 18.	Silty clay

Specimen	Areal Location	Stratigraphic Position	Lithology
7003	T. 134 N., R. 101 W., sec. 15, ne. 1/4, ne. 1/4, Slope County.	North end of Chalky Buttes; 15 feet below Golden Valley-Chadron contact; locality 18.	Analcimolite
6995	T. 134 N., R. 101 W., sec. 15, ne. 1/4, ne. 1/4, Slope County.	North end of Chalky Buttes; 15 feet below Golden Valley-Chadron contact; locality 18.	Analcimolite
4684	T. 137 N., R. 102 W., sec. 18, ne. 1/4, sw. 1/4, Billings Co.	Northeast corner of Bullion Butte; 10 feet below summit of butte; locality 14.	Arkose
7016	T. 137 N., R. 102 W., sec. 18, ne. 1/4, sw. 1/4, Billings Co.	Northeast corner of Bullion Butte; base of section; locality 14.	Arkose
4772	T. 137 N., R. 102 W., sec. 7 sw. 1/4, se. 1/4, Billings Co.	Northeast corner of Bullion Butte; base of section; locality 14.	Arkose
4776	T. 137 N., R. 102 W., sec. 18, nw. 1/4, sw. 1/4, Golden Valley Co.	West side of Bullion Butte; summit of butte; locality 15.	Arkose
4771	T. 137 N., R. 102 W., sec. 18, nw. 1/4, sw. 1/4, Golden Valley Co.	West side of Bullion Butte: 5 feet below summit of butte; locality 15.	Arkose
4781	T. 137 N., R. 102 W., sec. 18, nw. 1/4, sw. 1/4, Golden Valley Co.	West side of Bullion Butte; 10 feet below summit of butte; locality 15.	Arkose

Specimen	Areal Location	Stratigraphic Position	Lithology
4783	T. 137 N., R. 102 W., sec. 18, ne. 1/4, sw. 1/4, Golden Valley Co.	West side of Bullion Butte; 12 feet below summit of butte; locality 15.	Arkose
7007	T. 137 N., R. 102 W., sec. 18, nw. 1/4, sw. 1/4, Billings Co.	South end of Bullion Butte; summit of butte; locality 16.	Analcimolite
4775	T. 137 N., R. 102 W., sec. 18, nw. 1/4, sw. 1/4, Billings Co.	South of Bullion Butte; 5 feet below summit of butte; locality 16.	Analcimolite
4779	T. 137 N., R. 102 W., sec. 18, nw 1/4, sw. 1/4, Billings Co.	South end of Bullion Butte; 10 feet below summit of butte; locality 16.	Arkose
4777	T. 137 N., R. 102 W., sec. 18, nw. 1/4, sw. 1/4, Billings Co.	South end of Bullion Butte; 15 feet below summit of butte; locality 16.	Arkose
4770	T. 137 N., R. 102 W., sec. 18, nw. 1/4, sw. 1/4, Billings Co.	South end of Bullion Butte; 20 feet below summit of butte; locality 16.	Arkose
4782	T. 137 N., R. 102 W., sec. 18, nw. 1/4, sw. 1/4, Billings Co.	South end of Bullion Butte; 25 feet below summit of butte; locality 16.	Arkose
4774	T. 137 N., R. 102 W., sec. 18, ne. 1/4, sw. 1/4, Billings Co.	South end of Bullion Butte; base of section; locality 16.	Arkose
5972	T. 139 N., R. 104 W., sec. 8, ne. 1/4, sw. 1/4, Golden Valley Co.	Northeast corner of Flat Top Butte; summit of butte; locality 11.	Arkose

Specimen	Areal Location	Stratigraphic Position	Lithology
4670	T. 139 N., R. 104 W., sec. 8, ne. 1/4, sw. 1/4, Golden Valley Co.	Northeast corner of Flat Top Butte; 3 feet below summit of butte; locality 11.	Arkose
4674	T. 139 N., R. 104 W., sec. 8, ne. 1/4, sw. 1/4, Golden Valley Co.	Northeast corner of Flat Top Butte; 5 feet below summit of butte; locality 11.	Arkose
4788	T. 139 N., R. 104 W., sec. 8, ne. 1/4, sw. 1/4, Golden Valley Co.	Northeast corner of Flat Top Butte; 15 feet below summit of butte; locality 11.	Arkose
4782	T. 139 N., R. 104 W., sec. 8, ne. 1/4, sw. 1/4, Golden Valley Co.	Northeast corner of Flat Top Butte; 25 feet below summit of butte; locality 11.	Arkose
4787	T. 139 N., R. 104 W., sec. 8, ne. 1/4, sw. 1/4, Golden Valley Co.	Northeast corner of Flat Top Butte; 40 feet below summit of butte; locality 11.	Arkose
4669	T. 139 N., R. 104 W., sec. 8, ne. 1/4, sw. 1/4, Golden Valley Co.	Northeast corner of Flat Top Butte; 45 feet below summit of butte; locality 11.	Arkose
4748	T. 139 N., R. 104 W., sec. 8, ne. 1/4, sw. 1/4, Golden Valley Co.	Northeast corner of Flat Top Butte; 55 feet below summit of butte; locality 11.	Arkose
4749	T. 139 N., R. 104 W., sec. 8, ne. 1/4, sw. 1/4, Golden Valley Co.	Northeast corner of Flat Top Butte; base of section; locality 11.	Arkose

Specimen	Areal Location	Stratigraphic Position	Lithology
4685	T. 139 N., R. 104 W., sec. 16, ne. 1/4, sw. 1/4, Golden Valley Co.	South end of Flat Top Butte; summit of butte; locality 12.	Arkose
4785	T. 139 N., R. 104 W., sec. 16, nw. 1/4, ne. 1/4, Golden Valley Co.	South end of Flat Top Butte; summit of butte; locality 12.	Arkose
4673	T. 139 N., R. 104 W., sec. 16, nw. 1/4, ne. 1/4, Golden Valley Co.	South end of Flat Top Butte; summit of butte; locality 12.	Arkose
4747	T. 139 N., R. 104 W., sec. 16, ne. 1/4, sw. 1/4, Golden Valley Co.	Southwest side of Flat Top Butte; 25 feet below summit of butte; locality 13.	Arkose
4671	T. 139 N., R. 104 W., sec. 16, nw. 1/4, ne. 1/4, Golden Valley Co.	Southwest side of Flat Top Butte; 60 feet below summit of butte; locality 13.	Arkose
4708	T. 139 N., R. 104 W., sec. 6, se. 1/4, sw. 1/4, Golden Valley Co.	Northwest corner of Sentinel Butte; summit of butte; locality 1.	Arkose
4692	T. 139 N., R. 104 W., sec. 6, se. 1/4, sw. 1/4, Golden Valley Co.	Northwest corner of Sentinel Butte; summit of butte; locality 1.	Arkose
4707	T. 139 N., R. 104 W., sec. 6, se. 1/4, sw. 1/4, Golden Valley Co.	Northwest corner of Sentinel Butte; summit of butte; locality 1.	Arkose

Specimen	Areal Location	Stratigraphic Position	Lithology
5882	T. 139 N., R. 104 W., sec. 8, se. 1/4, sw. 1/4, Golden Valley Co.	Northwest side of Sentinel Butte; 10 feet below summit of butte; locality 1.	Arkose
4680	T. 139 N., R. 104 W., sec. 8, se. 1/4, sw. 1/4, Golden Valley Co.	Northwest side of Sentinel Butte; 10 feet below summit of butte; locality 1.	Arkose
4705	T. 139 N., R. 104 W., sec. 8, se. 1/4, sw. 1/4, Golden Valley Co.	Northwest side of Sentinel Butte; 12 feet below summit of butte; locality 1.	Arkose
5975	T. 139 N., R. 104 W., sec. 8, se. 1/4, sw. 1/4, Golden Valley Co.	Northwest side of Sentinel Butte; 15 feet below summit of butte; locality 1.	Arkose
7009	T. 139 N., R. 104 W., sec. 8, se. 1/4, sw. 1/4, Golden Valley Co.	Northwest side of Sentinel Butte; base section; locality 1.	Arkose
7014	T. 139 N., R. 104 W., sec. 8, nw. 1/4, nw. 1/4, Golden Valley Co.	North side of Sentinel Butte; summit of butte; locality 2.	Arkose
5970	T. 139 N., R. 104 W., sec. 8, nw. 1/4, nw. 1/4, Golden Valley Co.	North side of Sentinel Butte; summit of butte; locality 2.	Arkose
4690	T. 139 N., R. 104 W., sec. 8, nw. 1/4, nw. 1/4, Golden Valley Co.	North side of Sentinel Butte; 15 feet below summit of butte; locality 2.	Arkose

Specimen	Areal Location	Stratigraphic Position	Lithology
4672	T. 139 N., R. 104 W., sec. 8, nw. 1/4, nw. 1/4, Golden Valley Co.	North side of Sentinel Butte; 30 feet below summit of butte; locality 2.	Arkose
5981	T. 139 N., R. 104 W., sec. 8, nw. 1/4, nw. 1/4, Golden Valley Co.	North side of Sentinel Butte; 65 feet below summit of butte; locality 2.	Arkose
7011	T. 139 N., R. 104 W., sec. 8, nw. 1/4, nw. 1/4, Golden Valley Co.	North side of Sentinel Butte; 70 feet below summit of butte; locality 2.	Arkose
4688	T. 139 N., R. 104 W., sec. 8, nw. 1/4, nw. 1/4, Golden Valley Co.	North side of Sentinel Butte; base of section; locality 2.	Arkose
4682	T. 139 N., R. 104 W., sec. 8, se. 1/4, nw. 1/4, Golden Valley Co.	Southeast corner of Sentinel Butte; summit of butte; locality 3.	Arkose
4681	T. 139 N., R. 104 W., sec. 8, se. 1/4, nw. 1/4, Golden Valley Co.	Southeast corner of Sentinel Butte; 5 feet below summit of butte; locality 3.	Arkose
4693	T. 139 N., R. 104 W., sec. 8, se. 1/4, nw. 1/4, Golden Valley Co.	Southeast corner of Sentinel Butte; 35 feet below summit of butte; locality 3.	Arkose
5976	T. 139 N., R. 104 W., sec. 8, se. 1/4, nw. 1/4, Golden Valley Co.	Southwest corner of Sentinel Butte; summit of butte; locality 4.	Arkose

Specimen	Areal Location	Stratigraphic Position	Lithology
7010	T. 139 N., R. 104 W., sec. 8, se. 1/4, nw. 1/4, Golden Valley Co.	Southwest corner of Sentinel Butte; summit of butte; locality 4.	Arkose
4686	T. 139 N., R. 104 W., sec. 8, se. 1/4, nw. 1/4, Golden Valley Co.	Southwest corner of Sentinel Butte; summit of butte; locality 4.	Arkose
4691	T. 139 N., R. 104 W., sec. 8, se. 1/4, nw. 1/4, Golden Valley Co.	Southwest corner of Sentinel Butte; summit of butte; locality 4.	Arkose
4679	T. 139 N., R. 104 W., sec. 8, se. 1/4, nw. 1/4, Golden Valley Co.	Southwest corner of Sentinel Butte; 15 feet below summit of butte; locality 4.	Arkose
4687	T. 139 N., R. 104 W., sec. 8, se. 1/4, nw. 1/4, Golden Valley Co.	Southwest corner of Sentinel Butte; 20 feet below summit of butte; locality 4.	Arkose
4678	T. 139 N., R. 104 W., sec. 8, se. 1/4, nw. 1/4, Golden Valley Co.	Southwest corner of Sentinel Butte; 25 feet below summit of butte; locality 4.	Arkose
4689	T. 139 N., R. 104 W., sec. 8, se. 1/4, nw. 1/4, Golden Valley Co.	Southwest corner of Sentinel Butte; 25 feet below summit of butte; locality 4.	Arkose
4685	T. 139 N., R. 104 W., sec. 8, se. 1/4, nw. 1/4, Golden Valley Co.	Southwest corner of Sentinel Butte; 30 feet below summit of butte; locality 4.	Arkose

Specimen	Areal Location	Stratigraphic Position	Lithology
4675	T. 139 N., R. 104 W., sec. 8, se. 1/4, nw. 1/4, Golden Valley Co.	Southwest corner of Sentinel Butte; base of section; locality 4.	Arkose
7008	T. 139 N., R. 104 W., sec. 6, se. 1/4, sw. 1/4, Golden Valley Co.	West side of Sentinel Butte; summit of butte; locality 6.	Arkose
7013	T. 139 N., R. 104 W., sec. 6, se. 1/4, sw. 1/4, Golden Valley Co.	West side of Sentinel Butte; summit of butte; locality 6.	Arkose

CHADRON FORMATION

Specimen	Areal Location	Stratigraphic Position	Lithology
5977	T. 139 N., R. 104 W., sec. 16, nw. 1/4, ne. 1/4, Golden Valley Co.	Central part, west half of Sentinel Butte; summit of butte; locality 7.	Siltstone
4694	T. 139 N., R. 104 W., sec. 8, sw. 1/4, nw. 1/4, Golden Valley Co.	Central part, east half of Sentinel Butte; summit of butte; locality 7.	Siltstone

ARIKAREE FORMATION (?)

Specimen	Areal Location	Stratigraphic Position	Lithology
4745	T. 147 N., R. 96 W., sec. 34, se. 1/4, sw. 1/4, Dunn Co.	Central part of South Killdeer Mountain; summit of butte; locality 24.	Limestone

Specimen	Areal Location	Stratigraphic Position	Lithology
5988	T. 147 N., R. 96 W., sec. 34, se. 1/4, sw. 1/4, Dunn Co.	Central part of South Killdeer Mountain; summit of butte; locality 24.	Limestone
5987	T. 147 N., R. 96 W., sec. 34, se. 1/4, sw. 1/4, Dunn Co.	Central part of South Killdeer Mountain; summit of butte; locality 24.	Limestone
4744	T. 147 N., R. 96 W., sec. 34, se. 1.4, sw. 1/4, Dunn Co.	Central part of South Killdeer Mountain; summit of butte; locality 24.	Limestone
4745	T. 147 N., R. 96 W., sec. 34, se. 1/4, sw. 1/4, Dunn Co.	East side of South Killdeer Mountain; summit of butte; locality 25.	Sandstone
4741	T. 147 N., R. 96 W., sec. 34, se. 1/4, sw. 1/4, Dunn Co.	East side of South Killdeer Mountain; summit of butte; locality 25.	Sandstone
4740	T. 147 N., R. 96 W., sec. 34, se. 1/4, sw. 1/4, Dunn Co.	East side of South Killdeer Mountain; 10 feet below summit of butte; locality 25.	Sandstone
4742	T. 147 N., R. 96 W., sec. 34, se. 1/4, sw. 1/4, Dunn Co.	East side of South Killdeer Mountain; 25 feet below summit of butte; locality 25.	Sandstone

REFERENCES

REFERENCES CITED

Alexander, L. and Klug, H.P., 1948, Basic Aspects of X-Ray Absorption: Analytical Chemistry, V. 20, pp. 886-889.

Bassett, D.C., Keller, A., and Mitsuhashi, S., 1963, New Features in Polymer Crystal Growth from Concentrated Solutions: Journal of Polymer Science, Pt. A, V. 1, pp. 763-788.

Bergstrom, John R., 1956, The General Geology of Uranium in Southwestern North Dakota: North Dakota Geological Survey, Investigation Number 23.

Beroni, Ernest P. and Bauer, Herman L., 1952, Reconnaissance for Uraniferous Lignites in North Dakota, South Dakota, Montana, and Wyoming: United States Department of Interior, TEI-123, p. 93.

Bradley, W.H., 1928, Zeolite Beds in the Green River Formation: Science, new series, v. 67, pp. 73-74.

Bramlette, M.N. and Posnjak, E., 1933, Zeolitic Alteration of Pyroclastics: American Mineralogist, v. 18, pp. 167-171.

Brown, Ervin, and Thayer, T.P., 1963, Low-Grade Mineral Facies in Upper Triassic and Lower Jurassic Rocks of the Aldrich Mountains, Oregon: Journal of Sedimentary Petrology, v. 33, pp. 411-425.

Campbell, A.S. and Fyfe, W.S., 1965, Analcite-Albite Equilibria: American Journal of Science, v. 263, pp. 807-816.

Carlson, C.G., 1969, Bedrock Geologic Map of North Dakota: North Dakota Geological Survey Misc. Map Number 19.

Carrigy, M.A. and Mellon, G.B., 1964, Authigenic Clay Mineral Cements in Cretaceous and Tertiary Sandstones: Journal of Sedimentary Petrology, v. 34, pp. 461-472.

Clayton, Lee, 1965, Gravel-Sand-Silt-Clay Analysis; North Dakota Geological Survey Procedure A 65: 6 p.

Coombs, D.S., 1954, The Nature and Alteration of Some Triassic Sediments from Southland Zealand: v. 80, pt. I, pp. 65-109.

_____, 1955, X-Ray Investigations of Wairikite and Non-Cubic Analcime: Mineralogical Magazine, v. 30, p. 699.

_____, Ellis, A.J., Fyfe, W.S., and Taylor, A.W., 1959, The Zeolite Facies with Comments on the Interpretation of Hydrothermal Synthesis; Geochimica and Cosmoschimic Acta, V. 17, pp. 53-107.

Crook, Keith, A., 1969, Analysis of Five Analcimes from North America in Whetten, J.T., and Coombs, D.S., The Composition of Analcime from Sedimentary and Burial Metamorphic Rocks: Geological Society American Bulletin, v. 78, pp. 269-278.

Deer, W.A., Howie, R.A., and Zussman, J., 1962, Rock-Forming Minerals: John Wiley and Sons, v. 1-5.

Deffeyes, Kenneth S., 1959, Zeolites in Sedimentary Rocks: Journal of Sedimentary Petrology, v. 29, pp. 602-609.

Denson N.M., Bachman, George O., and Zeller, Howard, D., 1959, Uranium-Bearing Lignite in Northwestern South Dakota and Adjacent States: United States Geological Survey Bulletic 1055-B, 309 p.

_____, and Gill, J.R., 1965, Uranium-Bearing Lignite and Carbonaceous Shales in the Southwestern Part of Williston Basin-- A Regional Study: United States Geological Survey Professional Paper 463, 75 p.

_____, 1969, New Evidence of Age Relationships of Possible Eocene Rocks in Southwestern North Dakota: United States Geological Survey Professional Paper 650-B, pp. 63-65.

Eugster, A.P., 1965, Gels Composed of Sodium-Aluminum Silicate, Lake Magadi, Kenya: Science, v. 161, pp. 160-163.

Folk, R.L., 1964, Petrology of Sedimentary Rocks: Hemphill's, 150 p.

Fredrickson, A.F. and Cox, J. E., 1954, Solubility of Albite in Hydrothermal Solutions: American Mineralogist, v. 39, pp. 738-750.

Friedman, I., 1951, Some Aspects of the System $H_2O-Na_2O-Al_2O_3SiO_2$: Journal of Geology, v. 59, pp. 19-31.

Fyfe, W.S., and McKay, D.S., 1962, Hydroxyl Ion Catalysis of the Crystallization of Amorphous Silica at $330°$ C. and Some Observations on the Hydrolysis of Albite Solutions: American Mineralogist, v. 47, pp. 83-89.

Garrels, Robert L. and Christ, Robert, R., 1965, Solutions, Minerals, and Equilibria: Harper and Row, 450 p.

Gaudette, H.E., 1965, Illite from Fon Du Lac County, Wisconsin: American Mineralogist, v. 50, pp. 411-417.

Goodwin, J.R. and Surdam, R.E., 1967, Zeolitization of Tuffaceous Rocks of the Green River Formation, Wyoming: Science, v. 157, pp. 307-308.

Grim, Ralph E., 1953, Clay Mineralogy: McGraw-Hill, 384 p.

Gulbrandsen, R.A. and Cressman, E.R., 1960, Analcime and Albite in Altered Jurrasic Tuff in Idaho and Wyoming: Journal of Geology, v. 68, pp. 458-464.

Hansen, Miller, 1956, Geologic Map of North Dakota: Misc. Map Number Two: North Dakota Geological Survey.

Harris, R.C., 1967, Silica and Chloride of Interstitial Waters of River and Lake Sediments: Limnology and Oceanography, v. 22, pp. 8-12.

Hay, Richard L., and Moiola, R.J., 1963, Authigenic Minerals in Searles Lake, California: Sedimentology, v. 7, pp. 327-340.

_____, 1966, Zeolites and Zeolitic Reactions in Sedimentary Rocks: Geological Society of America Special Paper, Number 85, 130 p.

Hemley, J.J., 1959, Some Mineralogical Equilibria in the System $K_2O-Al_2O_2-SiO_2-H_2O$: American Journal of Science, v. 257, pp. 241-270.

Hess, Paul C., 1966, Phase Equilibria of Some Minerals in the $K_2O-Na_2O-A_{22}O_3-SiO_2-H_2O$ at 25 C. and 1 Atmosphere Pressure: American Journal of Science, v. 264, pp. 289-309.

Hickey, Leo J., 1962, The Paleobotany and Stratigraphy of the Golden Valley Formation in Southwestern North Dakota: Unpublished Ph.D. Dissertation, Princeton University, 265 p.

Ijima, A., and Utada, M., 1966, Zeolites in Sedimentary Rocks with Reference to Depositional Environments: Sedimentology, v. 7, pp. 327-330.

_____, and Hay, R.L., 1968, Analcime Composition in Tuffs of the Green River Formation of Wyoming: American Mineralogist, v. 53, pp. 184-200.

Karner, Frank, R., 1968, in North Dakota Geological Survey Report of Investigations Number 48, 41 p.

Keller, W.D., 1952, Analcime in the Popo Agie Member of the Chugwater Formation: Journal of Sedimentary Petrology, v. 22, pp. 70-82.

_____, Balgord, W.D., and Reesman, A., 1963, Dissolved Products of Artificially Pulverized Silicate Minerals and Rocks--Pt. I: Journal of Sedimentary Petrology, v. 33, pp. 191-204.

Klug, Harold P. and Alexander, LeRoy R., 1954, X-Ray Diffraction Procedures: John Wiley and Sons, Inc., 716 p.

Krumbein, W.C. and Sloss, L.L., 1963, Stratigraphy and Sedimentation: W.M. Freeman and Company, 600 p.

Laird, Wilson, M., and Towse, Donald F., 1951, Stratigraphy in North Dakota with Reference to Oil Possibilities: North Dakota Geological Survey Report of Investigations, 2 sheets.

Leonard, A.G., 1908, Fifth Biennal Report: North Dakota Geological Survey, 278 p.

_____, 1911, The Cretaceous and Tertiary Formations of Western North Dakota and Eastern Montana: Journal of Geology, v. 19, pp. 507-548.

Leroux, Jean, Lennox, D.H., and Kay, Kingsley, 1953, Direct Quantitative X-Ray Analysis: Analytic Chemistry, v. 25, pp. 740-743.

Livingstone, D.A., 1963, Chemical Composition of Rivers and Lakes in Data of Geochemistry: United States Geological Survey Professional Paper 440-G, 64 p.

Loughnan, F.C., 1964, A Comparative Study of the New Castle and Illawarra Coal Measure Sediments of the Sidney Basin, New South Wales: Journal of Sedimentary Petrology, v. 36, pp. 1016-1025.

Magill, T.H., 1965, Spherulitic Crystallization Pt. I. "Odd-Even" Polymides: Nylon 56 and Nylon 96: Journal of Polymer Science, Pt. A, v. 3, pp. 1195-1219.

Meek, F.B. and Hayden, F.V., 1858, Descriptions of New Species of Genera of Fossils Collected by Dr. F.V. Hayden in Nebraska Territory; with some Remarks on the Tertiary and Cretaceous Formations of the Northwest: Philadelphia Academy of Natural Sciences Proceedings. 1857, v. 9, pp. 117-133.

Morey, G.W. and Chen, W.T., 1955, The Action of Hot Water on Some Feldspars: American Mineralogist, v. 40, pp. 996-1000.

_____, and Fournier, R.O., 1961, The Decomposition of Microcline, Albite, and Nepheline in Hot Water: American Mineralogist, v. 46, pp. 688-699.

Moore, George, W., Melin, Robert E., and Kepferle, Roy C., 1959, Uranium-Bearing Lignite in Southwestern North Dakota: United States Geological Survey Bulletin 1055-E, pp. 147-166.

Niskansen, Eric, 1964, Quantitative Mineral Analysis of Kaolin-Bearing Rocks by X-Ray Diffraction: Analytic Chemistry, v. 36, pp. 1268-1270.

Saha, P., 1959, Geochemical and X-Ray Diffraction Investigation of Natural and Synthetic Analcites: American Mineralogist, v. 44, pp. 300-313.

_____, 1961, The System $NaAlSiO_4$ (Nepheline)-$NaAlSi_3O_8$ (Albite)-H_2O: American Mineralogist, v. 46, pp. 859-884.

Sand, L.B., Roy, and Osborn, E.F., 1957, Stability Relations of Some Minerals in the $Na_2O-Al_2O_3-SiO_2-H_2O$ System: Economic Geology, v. 52, pp. 169-179.

Sears, Gerald W., 1961, The Origin of Spherulites: Journal of Physical Chemistry, v. 65, pp. 1738-1741.

Tatlock, D.B., 1966 Rapid Modal Analysis of Some Felsic Rocks from Calibrated X-Ray Diffraction Patterns: U.S. Geological Survey Bulletin 1209, 41 p.

Turner, F.J., 1958, Mineral Assemblages of Individual Metamorphic Facies in Metamorphic Reactions and Metamorphic Facies: Geological Society of America Memoir 73, 259 p.

Van Houten, R.B., 1962, Cyclic Sedimentation and the Origin of Analcime-Rich Upper Triassic Lockatong Formation, West Central New Jersey and Adjacent Pennsylvania: American Journal of Science, v. 260, pp. 561-576.

Velde, B., and Hower, J., 1963, Petrological Significance of Illite Polymorphism in Paleozoic Sedimentary Rocks: American Mineralogist, v. 48, pp. 1239-1254.

Wahlstrom, Ernest E., 1960, Petrographic Mineralogy: John Wiley and Sons, Inc., 408 p.

Wanless, A.R., 1922, Lithology of the White River Sediments: American Philosophical Society Proceedings, v. 61, pp. 181-203.

Whetten J.T. and Coombs, D.S., 1967, The Composition of Analcime from Sedimentary and Burial Metamorphic Rocks: Geological Society of America Bulletin, v. 78, pp. 269-278.

Wilkinson, J.F.G. and Whetten, J.T., 1964, Some Analcime-Bearing Pyroclastics and Sedimentary Rocks from New South Wales: Journal of Sedimentary Petrology, v. 34, pp. 543-553.

_____, 1968, Analcimes from Some Potassic Igneous Rocks and Aspects of Analcime Igneous Assemblages: Contributions to Mineralogy and Petrology: v. 18, pp. 252-270.

Zussman, J., 1967, X-Ray Diffraction in Physical Methods in Determination Mineralogy, ed. J. Zussman: Academic Press, 514 p.